

Depth-Based Local Center Clustering: A Framework for Handling Different Clustering Scenarios

Siyi Wang, Alexandre Leblanc, Paul D. McNicholas

Abstract—Cluster analysis, or clustering, plays a crucial role across numerous scientific and engineering domains. Despite the wealth of clustering methods proposed over the past decades, each method is typically designed for specific scenarios and presents certain limitations in practical applications. In this paper, we propose depth-based local center clustering (DLCC). This novel method makes use of data depth, which is known to produce a center-outward ordering of sample points in a multivariate space. However, data depth typically fails to capture the multimodal characteristics of data, something of the utmost importance in the context of clustering. To overcome this, DLCC makes use of a local version of data depth that is based on subsets of data. From this, local centers can be identified as well as clusters of varying shapes. Furthermore, we propose a new internal metric based on density-based clustering to evaluate clustering performance on non-convex clusters. Overall, DLCC is a flexible clustering approach that seems to overcome some limitations of traditional clustering methods, thereby enhancing data analysis capabilities across a wide range of application scenarios.

Index Terms—Clustering, statistical depth, similarity matrix, Mahalanobis depth, spatial depth, internal metric.

I. INTRODUCTION

Clustering, or cluster analysis, is one of the most important topics in data science. A cluster is usually seen as a set of similar objects that have been gathered or grouped together [1]. Generally speaking, clustering is the task of partitioning a collection of objects, into separate clusters, in such a way that objects in the same cluster are as similar as possible and objects in separate clusters as distinct as possible [2]. Research on clustering methods has a long history in several disciplines, including biology, psychology, geography, and marketing [3]. In recent years, the rapid development of sensing and storage technology has resulted in the collection of vast quantities of high-dimensional, large-scale, data. In turn, this has increased the need for flexible and computationally efficient clustering methods [4] in many fields, such as pattern recognition [5], computer vision [6], [7] and image processing [8].

The complexity of data distributions has led to the development of numerous clustering algorithms, each having a unique set of strengths and constraints. We next briefly discuss different traditional clustering methods to highlight their distinct characteristics and limitations. In this, and in

what follows, we consider the objects to be clustered as points in the d dimensional real space \mathbb{R}^d .

A. Clustering Methods

1) Center-Based Clustering: Center-based clustering methods, with k-means clustering [9] being a prime example, are often utilized due to their simplicity and effectiveness. However, k-means clustering has several limitations. Firstly, it is sensitive to outliers as it uses the means of the points in each cluster as cluster centers. Secondly, even in outlier-free contexts, this approach is most adequate when clusters are spherically symmetric, which may not always be representative of the actual data distribution. Lastly, the algorithm is sensitive to initialization and can easily get trapped in local minima. To address some of these issues, several variants of the k-means algorithm have been developed:

- Partitioning around medoids (PAM; [10]), was introduced to combat the sensitivity to outliers. Instead of cluster means, PAM uses medoids (a form of multivariate median) as cluster centres.
- Weighted k-means (W-k-means; [11]) and lasso weighted k-means (LW-k-means; [12]) were designed to address the underlying spherical symmetry assumption for clusters. These both provide a more flexible k-means approach by incorporating a weight vector for each variable. LW-k-means improves W-k-means by adding a lasso penalty to the objective function, enabling feature selection in high-dimensional data.
- Power k-means [13] and kernel power k-means [14] were developed to address the sensitivity of k-means to initialization and tendency to get trapped in local minima by redefining the objective function using power means. Kernel power k-means extends this by incorporating multiple kernel configurations to handle non-linear separable data via higher-dimensional projections.

2) Density-Based and Hierarchical Clustering: Density-based clustering assumes that clusters are regions of high density separated by low-density areas, making it well-suited for detecting arbitrarily shaped clusters. For instance, density-based spatial clustering of applications with noise (DBSCAN; [15]) sets a threshold and minimum point count for a region to be considered dense. Then, dense regions that can be directly connected with each other are merged into a cluster. However, DBSCAN's reliance on a fixed threshold limits its ability to handle clusters with varying densities.

Hierarchical clustering, on the other hand, adopts a tree-like approach to iteratively merge or split clusters. It offers

S. Wang is a Ph.D. candidate and P.D. McNicholas is the Canada Research Chair in Computational Statistics at the Dept. of Mathematics and Statistics, McMaster University, Hamilton, ON, Canada. A. Leblanc is a Professor at the Dept. of Statistics, University of Manitoba, Winnipeg, MB, Canada. E-mail: {wangs424,paulmc}@mcmaster.ca, alex.leblanc@umanitoba.ca
Code is available at <https://github.com/lytgystrn/dlcc>

two main strategies: agglomerative (bottom-up) and divisive (top-down). The resulting dendrogram represents cluster relationships, from an all-inclusive cluster at the top to individual objects at the bottom [16]. While hierarchical clustering provides an intuitive structure, its high computational cost and irreversible decisions make it less suitable for large datasets or complex cluster shapes.

Density peak clustering (DPC) [17], introduced in 2014, takes a different approach by combining density and distance to identify cluster centers. It locates density peaks based on a decision graph, where density is plotted on the y-axis and the distance to the nearest higher-density point on the x-axis. This method allows for manual selection of cluster centers and performs well with varying-density clusters. However, it can struggle with robustness, as density peaks may correspond to satellite points rather than true cluster centers.

An improved version, fast main density peak clustering within relevant regions (R-MDPC) [18], proposed in 2024, incorporates hierarchical concepts by applying single-linkage clustering to density peaks, defining relevant regions as density-connected areas. This enhancement better handles complex cluster shapes by merging single-density peak clusters and reducing satellite peak interference. However, for highly overlapping or extremely high-dimensional datasets, R-MDPC may collapse all points into one region, behaving similarly to the original DPC.

3) *Model-Based Clustering*: Model-based clustering typically assumes the points to be clustered stem from an underlying mixture distribution [19], whose components are naturally associated with the clusters to be constructed. For example, working from a Gaussian mixture model (GMM), one can identify elliptical clusters with varying orientations, shapes, and sizes. Other mixture models handling asymmetric distributions have also been developed, see, e.g., [20], [21], [22], and [23]. These different families of mixture models lead to clustering methods typically relying on the expectation-maximization (EM) algorithm [24] to find optimal parameter values, which can be computationally intensive. Moreover, selection of the most appropriate family of mixture models can be challenging unless knowledge about the data-producing mechanism and/or subject area expertise is available.

4) *Spectral and Subspace Clustering*: Spectral clustering [25], a notable graph-based method, treats clustering as a graph partitioning problem, converting data points into nodes and their similarities into connecting edge weights. It is well-suited for high-dimensional datasets, often utilizing a sparse adjacency matrix derived from the k-nearest neighbors methods. After representing the data as a similarity graph, the clustering problem can essentially be seen as partitioning the graph in such a way that edges between groups are given low weights and edges within groups high weights [26].

Spectral clustering has been extended and has led to other clustering techniques. It is, for instance, an essential component of modern subspace clustering algorithms. These algorithms have gained attention due to their capacity for identifying low-dimensional representations of high-dimensional data [27]. In particular, sparse subspace clustering (SSC) [28] is a key evolution in this domain. Making use of the

self-expressiveness property, points are expressed as linear combinations of other points within the same subspace. Therefore, SSC merely requires the coefficient matrix of these linear combinations. As a result, SSC overcomes two major challenges of spectral clustering: selecting an appropriate neighborhood size and handling points near the intersection of two subspaces. However, for low-dimensional data, the premise that data points can be effectively represented as linear combinations of the lower-dimensional subspace may falter, potentially leading to a diminished efficacy of SSC. This makes SSC a tool that is primarily designed for high-dimensional datasets.

B. Motivation

Our objective is to develop a versatile clustering framework capable of addressing diverse challenges, from convex to non-convex cluster shapes, and from low- to high-dimensional data. A common theme across clustering methods is their reliance on representative points, or exemplars. Center-based methods define exemplars by minimizing within-cluster distances, often relying on distance metrics. However, a specific distance measure often performs well only for certain types of data, and adapting to more diverse structures may require mapping data into higher-dimensional spaces via kernel methods. The effectiveness of such approaches, however, hinges on selecting an appropriate kernel, which can be challenging and highly sensitive to the data. Density-based methods, on the other hand, define exemplars through local density variations. These methods identify clusters by connecting dense regions, but the appropriate definition of density often depends on the dimensionality of the data. For example, density measures that work well in low-dimensional spaces may lose effectiveness in high-dimensional settings due to the sparsity of data. Moreover, in overlapping regions, density connections often struggle to distinguish between clusters. Both center-based and density-based approaches share a reliance on exemplars but are inherently limited by their respective definitions of exemplars.

A versatile clustering framework must overcome these limitations by introducing an adaptive similarity measure that avoids strong parametric assumptions and generalizes across diverse data geometries. Equally important is the need for a robust exemplar definition that is consistent across dimensions and cluster shapes, along with effective grouping strategies for these exemplars to form meaningful clusters.

In response, our method introduces a more flexible exemplar definition by leveraging statistical data depth, a nonparametric tool for multivariate analysis. Tukey [29] pioneered the idea of center-outward ordering in multivariate data, with the introduction of the first depth definition, half-space depth. Data depth enables the center-outward ordering of data, making it a potent tool for locating a center for any dataset. When considering subsets of the data, data depth with respect to each subset aids in defining multiple exemplars. Naturally, as the subset size grows, the number of exemplars diminishes, and vice versa.

Building on this concept, we propose the depth-based local center clustering (DLCC) algorithm. Equipped with two grouping strategies for depth-defined representative points,

DLCC inherits strengths from both center-based and density-based methods, while offering greater flexibility to tackle a wide range of clustering problems. Here, the term “depth-based” encompasses two aspects: (1) data depth is used to construct a similarity matrix instead of relying on distance, adaptively capturing the geometric characteristics of each point’s location; (2) data depth measures the centrality of points within each point’s neighborhood, helping to identify exemplars.

Furthermore, ground truth is typically not available in real-world clustering applications, necessitating the use of internal metrics to evaluate performance. Established metrics like the average silhouette width (ASW; [49]), which measures the average distance within clusters relative to the nearest cluster, and the Calinski-Harabasz index (CHI; [50]), which relies on distances from points to their cluster centroids, inherently favor spherical clusters. This preference limits their effectiveness in capturing non-convex shapes, as illustrated in Figure 1, where they will incorrectly favor clustering result (c) over (a). To address these shortcomings, we propose a new internal metric, the depth-based clustering (DC) metric, designed to more accurately handle complex cluster shapes and assist in parameter selection for our algorithm. Further details will be discussed in Section IV-B.

C. Main Contributions and Organization of the Paper

This paper makes the following main contributions:

- **Depth-Based Similarity Matrix:** We improve the efficiency when constructing a depth-based similarity matrix using Mahalanobis depth (MD) and Spatial depth (SD). For the MD-based similarity matrix, model-based clustering methods are employed to predefine covariance matrices that approximate the data’s distribution shapes. For the SD-based similarity matrix, we develop an efficient matrix-based computation method.
- **DLCC Clustering Framework:** We develop a novel clustering framework, DLCC, which includes the definition of a similarity measure and local centers, and the introduction of methods for filtering and grouping local centers. Experiments shows it achieves competitive performance across different types of clustering challenges among the representative algorithms from each type of clustering method referenced in Section I-A.
- **Internal Evaluation Metric:** We propose a depth-based clustering metric as an internal evaluation criterion. This metric combines the density-based clustering concept with the depth-based similarity matrix to evaluate clustering performance, particularly for non-convex cluster structures.

The remainder of the paper is organized as follows: Section II reviews key concepts of data depth and introduces the depth-based similarity matrix. Section III provides a detailed description of the DLCC framework. In Section IV, we discuss the hierarchical structure of DLCC and present the proposed internal metric for parameter selection. Section V showcases experimental results of DLCC using both synthetic and real-world datasets. Lastly, Section VI concludes the paper.

Figure 2 provides the flowchart of the DLCC method, and Table I summarizes the key notations used in this paper to help readers navigate its contents more easily. Additional graphs providing further insights into our methods are included in the supplementary file.

TABLE I: Summary of the main notations

Notation	Description
n and d	Number of observations and dimensions, respectively;
$D_{\text{MD/SD}}(\mathbf{z} \mathbf{X})$	Mahalanobis or spatial depth of \mathbf{z} with respect to \mathbf{X} ;
\mathbf{X}	A given dataset;
\mathbf{X}_{Ri}	Dataset reflected around \mathbf{x}_i , i.e., $\mathbf{X}_{Ri} = \mathbf{X} \cup \{2\mathbf{x}_i - \mathbf{x}_j \mid j \neq i\}$;
$\mathbf{E}, \bar{\mathbf{E}}$	Matrices of unit vector sums from \mathbf{X} and reflected points to \mathbf{X} ;
\mathbb{S}	Depth-based similarity matrix, with \mathbb{S}_{ij} its ij -th entry;
s	Neighborhood size;
\mathbf{N}_i	Depth-based neighborhood of \mathbf{x}_i ;
$r_i(\mathbf{x}_j)$	Depth rank of \mathbf{x}_j within \mathbf{N}_i ;
$c, \mathbf{c}, \mathbf{C}$	A local center, a certain set of local centers, and the set of all filtered centers, respectively;
\mathbb{M}	Local center neighborhoods’ similarity matrix, with \mathbb{M}_{ij} its ij -th entry;
δ	Similarity threshold for local center grouping (\mathbb{M} -based);
\mathbf{g}	A group of local centers;
\mathbf{U}_g	Unique neighbors of group \mathbf{g} ;
G and K	Number of groups and clusters, typically $G = K$;
k	Cluster index;
\mathcal{X}_k	Observations in cluster k ;
f	Frequency of a local center;
\mathcal{P}	Cumulative proportion of neighbors of local centers to all points;
S_k, \hat{S}_k	Score pools for accepting and leaving points unlabelled in cluster k ;
η_k, η_X	Depth similarity thresholds for cluster k and the dataset (\mathbb{S} -based);
\mathcal{I}_k	Indices of points in \mathbf{g}_k ;
\mathcal{J}_k^i	Indices of core neighbors of \mathbf{x}_i in \mathcal{X}_k based on η_k ;
\mathcal{H}_k^i	Indices of core neighbors of \mathbf{x}_i outside \mathcal{X}_k based on η_X ;
\mathbf{I}_k	Inner observations of cluster k ;
\mathbf{O}_k	DBCA-outliers of cluster k ;

II. DEPTH-BASED SIMILARITY MATRIX

A. Preliminaries

A depth function quantifies how “central” a point is within a multidimensional data distribution, providing a meaningful center-outward ordering of points. The term “depth” reflects the analogy to physical depth: points closer to the “central area” of a distribution are considered “deeper”, while points farther away are “shallower”. It is worth to note that a point with high depth is central but does not necessarily coincide with a region of high density. Consequently, clustering approaches based on depth are conceptually distinct from those based on density estimates. This centrality-based ordering is particularly useful in multivariate data analysis, where traditional univariate notions of order are not well-defined.

Serfling and Zuo [30] formulated several desirable properties of depth functions: affine invariance, maximality at center, monotonicity on rays, and vanishing at infinity. A deepest point $\mathbf{m} = \operatorname{argmax}_{\mathbf{z} \in \mathbb{R}^d} D(\mathbf{z} \mid F)$ is usually referred to as a depth median. In applications, where the inherent distribution F is usually unknown, depth is calculated with respect to the empirical distribution F_n of \mathbf{X} , that is $D(\mathbf{z} \mid F_n)$ is the depth of \mathbf{z} with respect to the sample \mathbf{X} . Hereinafter, we will denote the latter as $D(\mathbf{z} \mid \mathbf{X})$ to emphasize the role of the sample on calculating the depth of the point \mathbf{z} . For a broader overview of various depth notions, see Mosler and Mozharovskiy [31].

Previous studies have explored the application of data depth in clustering. Jornsten [32] proposed DDclust, an algorithm

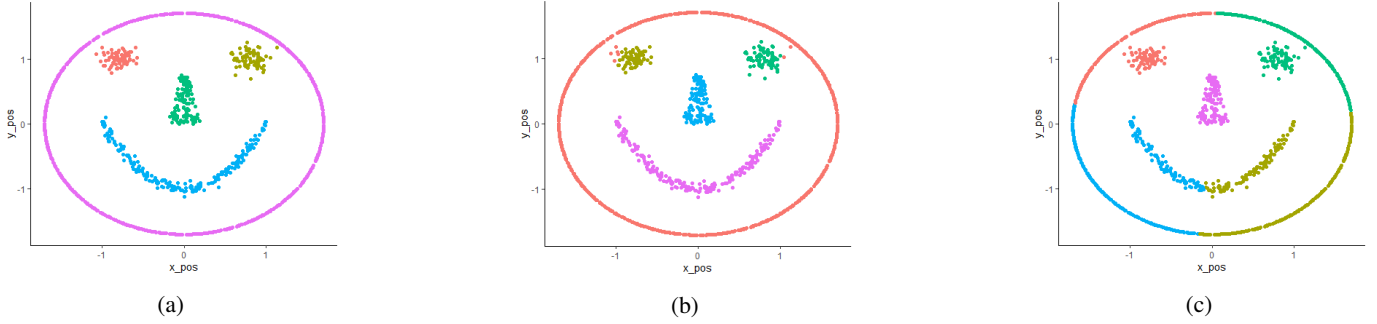


Fig. 1: Clustering results for the synthetic dataset SmileyF. Panel (a) shows the ground truth, (b) misclusters several points in the eyes, and (c) fails to capture the face pattern.

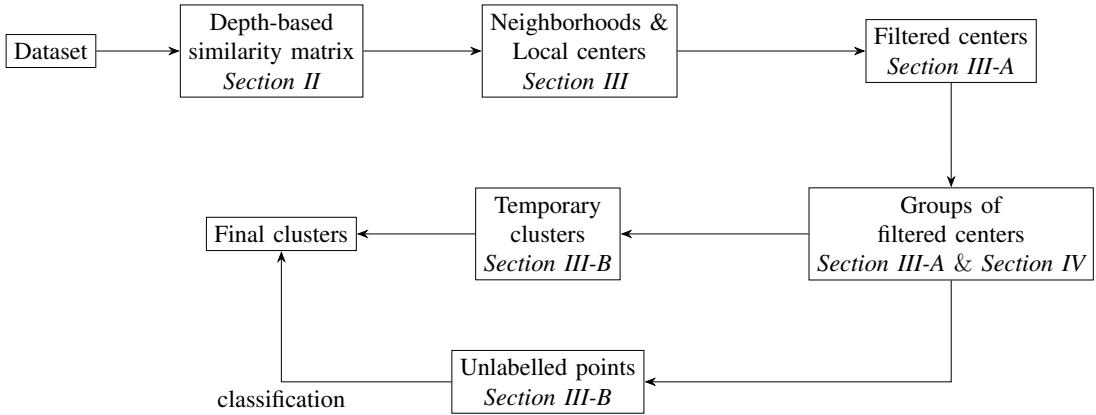


Fig. 2: Flowchart for the DLCC algorithm, detailing the sections that include the key contents represented in the nodes.

that refines the output of other clustering methods like PAM by recalculating observation depths within each cluster and re-allocating points for better results. Jeong et al. [33] introduced data depth-based clustering analysis (DBCA), an alternative to DBSCAN. DBCA replaces the sample Mahalanobis depth (MD) function

$$D_{MD}(\mathbf{z} | \mathbf{X}) = \left[1 + (\mathbf{z} - \bar{\mathbf{X}})' \hat{\Sigma}^{-1} (\mathbf{z} - \bar{\mathbf{X}}) \right]^{-1} \quad (1)$$

with fixed depth median versions

$$D_{MD}^i(\mathbf{z}) = \left[1 + (\mathbf{z} - \mathbf{x}_i)' \hat{\Sigma}^{-1} (\mathbf{z} - \mathbf{x}_i) \right]^{-1}, \quad (2)$$

where \mathbf{z} denotes a point in \mathbb{R}^d , $\bar{\mathbf{X}}$ is the mean vector, \mathbf{x}_i is an observation in \mathbf{X} , while $\hat{\Sigma}$ is the estimated covariance matrix of dataset \mathbf{X} . Unlike DBSCAN, which uses fixed Euclidean distance for neighborhoods, DBCA employs (2) to define elliptical, affine-invariant neighborhoods. Recent work has also explored data depth to identify centroids for k-means initialization in diverse datasets [34], [35].

So far, the notion of depth serves an auxiliary role to the more traditional clustering methods and is not employed directly in examining the multimodality of data. Herein, two depth functions are considered for our DLCC algorithm: MD and spatial depth (SD). For SD [36], the sample version is

$$D_{SD}(\mathbf{z} | \mathbf{X}) = 1 - \left\| \sum_{i=1}^n \frac{\mathbf{z} - \mathbf{x}_i}{n \|\mathbf{z} - \mathbf{x}_i\|} \right\|, \quad (3)$$

where n is the total number of observations. Although SD is only invariant under similarity transformations, it is nevertheless a sensible choice in the current context due to its straightforward computation in high-dimensional spaces.

DLCC requires a similarity matrix to determine the neighbors of each observation. Traditional distance measures, such as Euclidean distance, are typically based on assumptions about the underlying cluster shapes (e.g., spherical or linear structures), which may not hold in more complex scenarios. In contrast, data depth offers a nonparametric, robust, and adaptive alternative. As the depths (1) and (3) provide a center-outward ordering and their value ranges from 0 to 1, the depth values of other points can be viewed as a measure of similarity to the depth median. Thus, similarity matrices can be constructed based on data depth. For this, however, one requires an approach capable of defining neighbors of any point \mathbf{x}_i in \mathbf{X} , i.e., the observations in \mathbf{X} that are most similar to \mathbf{x}_i . It should be clear that the usual notion of depth cannot be applied directly here, as that can only provide similarity measurements related to the global median.

Now, consider a point \mathbf{x}_i in \mathbf{X} whose neighbors need to be identified and introduce the set

$$\mathbf{X}_{Ri} = \mathbf{X} \cup \{2\mathbf{x}_i - \mathbf{x}_j \mid j \neq i, j = 1, 2, \dots, n\}.$$

We note that this new set is comprised of all the points belonging to the original sample \mathbf{X} as well as of the reflection of all the points of \mathbf{X} through \mathbf{x}_i . Crucially, \mathbf{x}_i is a depth median

of \mathbf{X}_{Ri} as it is a center of symmetry for this set. It is also the case that $D(\mathbf{x}_i|\mathbf{X}_{Ri}) = 1$ and that $D(\mathbf{x}_j|\mathbf{X}_{Ri})$ can be used to quantify the similarity of any point \mathbf{x}_j ($j \neq i$) to the point of interest \mathbf{x}_i . Subsequently, by repeatedly computing the depth values for points in \mathbf{X} with respect to $\mathbf{X}_{R1}, \mathbf{X}_{R2}, \dots, \mathbf{X}_{Rn}$, a $n \times n$ non-mutual depth-based similarity matrix can be defined. We denote it as \mathbb{S} , where $\mathbb{S}_{ij} = D(\mathbf{x}_j|\mathbf{X}_{Ri})$ represents the entry in the i th row and j th column. As will be seen shortly, this can cause some computational challenges.

This approach to localize the concept of depth was introduced by Paindaveine and Van Bever [37] when they introduced local depth, which was shown to yield non-spherical depth neighborhoods in some contexts. The same authors [38] used this concept and introduced an affine-invariant k-nearest neighbor classification algorithm that adapts to the local geometry of the sample and was shown to be consistent.

B. Mahalanobis Depth based Similarity Matrix

Previous studies [39] have employed the approach of using individual observations \mathbf{x}_i , $i = 1, 2, \dots, n$, in place of the mean vector, while incorporating the globally estimated covariance matrix, for depth value computations as given in (2). In other words, the center used for calculating the Mahalanobis depth is shifted to each observation, and the depth values of the remaining observations are subsequently recorded. These studies commonly employ the minimum covariance determinant (MCD) method [40] to achieve robust results. In light of the previous discussion, the mean of \mathbf{X}_{Ri} can easily be seen to be \mathbf{x}_i , which leads to

$$D_{\text{MD}}(\mathbf{z} | \mathbf{X}_{Ri}) = D_{\text{MD}}^i(\mathbf{z}),$$

assuming the use of a consistent covariance matrix. This implies that making use of (2) to define a neighborhood of any point is in line with the approach of Paindaveine and Van Bever.

However, the method of Paindaveine and Van Bever necessitates estimating n distinct covariance matrices, substantially increasing computational load. In contrast, the DBCA approach estimates only a single global covariance matrix, which may not adequately reflect the diversity within different clusters. To mediate between these extremes, we propose a covariance matrix selection strategy that balances computational efficiency with the ability to capture the unique characteristics of each cluster more effectively than a global approach.

In the framework of GMM, it is feasible to estimate multiple covariance matrices, ideally keeping the number of such matrices less than or equal to the number of clusters — substantially fewer than n — yet more than one. The covariance matrix for cluster k , i.e., component k , can be decomposed as

$$\Sigma_k = \lambda_k \Gamma_k \Delta_k \Gamma_k', \quad (4)$$

where $\lambda_k = |\Sigma_k|^{1/d}$, Γ_k denotes the matrix of eigenvectors, and Δ_k is a diagonal matrix of eigenvalues with the condition $|\Delta_k| = 1$ [41], [42]. These elements, respectively, represent size, orientation, and shape of the cluster; see [43] for details.

In our study, we focus on the EEV model from the Gaussian parsimonious clustering models (GPCM) family, wherein

different clusters estimated by the EEV model share common λ_k and Δ_k — i.e., $\lambda_k = \lambda$ and $\Delta_k = \Delta$ — but possess distinct Γ_k . When model performance metrics, such as the Bayesian information criterion (BIC; [44]), are similar for results with varying numbers of components, those with fewer components are preferred. We do not consider more flexible models within the GPCM family as these could result in GMMs that overfit the data, and the size of the estimated covariance matrices may be too small for constructing the similarity matrix.

If we assume clusters are all convex, we use a test based on principal component analysis (PCA; [45]) to decide on the method for constructing the similarity matrix. With the close correlation between the Mahalanobis distance and PCA, the squared Mahalanobis distance is equal to the sum of squares of standardized principal component scores [46]. If a significant proportion of variance can be explained by the leading principal components, then the Mahalanobis distance in the space spanned by these components is a suitable metric, especially in the presence of strong inter-variable correlations. In contrast, if the variables show no clear correlations, the standard Euclidean distance is deemed a more appropriate measure.

The test procedure can be summarized as follows: Let $\mathbf{vp} = \{vp_1, vp_2, \dots, vp_H, \dots, vp_d\}$, which contains the proportion of variance explained by each PC from high to low, where H indicates the number of PCs that explain over 5% variance, but if $H = d$, then H redefined to be $d - 1$. If either (5) or (6) is satisfied, the dataset passes the test:

$$vp_1 > 0.6, \quad (5)$$

$$\sum_{h=1}^H vp_h > 0.95. \quad (6)$$

When the dataset passes the test, we use the estimated global covariance matrix. If it fails, the EEV model is brought into play, offering the benefit of estimating clusters with identical eigenvalues. The test can be repeated using the eigenvalues derived from the EEV model. If it continues to fail, indicating weak inter-variable correlations even within clusters, and the Euclidean distance becomes sufficient for constructing the similarity matrix, setting the covariance matrix in (2) as the identity matrix. However, if it succeeds, suggesting the presence of within-cluster correlations, we employ the covariance matrices estimated by the EEV model. Specifically, consider two points, \mathbf{x}_i and \mathbf{x}_j , where \mathbf{x}_i is assigned to cluster 1 and \mathbf{x}_j to cluster 2 by the EEV model. The estimated covariance matrices, $\hat{\Sigma}_1$ for cluster 1 and $\hat{\Sigma}_2$ for cluster 2, are used to compute the i th and j th rows of the similarity matrix, respectively. While both covariance matrices are of the same size and shape, their orientations differ to capture the inter-variable correlation within each cluster.

C. Spatial Depth based Similarity Matrix

A spatial-depth-based similarity matrix can be constructed from calculating $D_{\text{SD}}(\mathbf{x}_j|\mathbf{X}_{Ri})$ for all $i, j = 1, 2, \dots, n$. One advantage of using this depth measure is that the shape of the resulting neighborhoods is determined by the local geometry

of the sample and does not rely on any parameters. This is a potentially very interesting advantage, but it does entail the computationally intensive process of repeatedly calculating depth values for the n sample points with respect to n distinct datasets $\mathbf{X}_{R1}, \mathbf{X}_{R2}, \dots, \mathbf{X}_{Rn}$. Hence, we delve into certain properties of spatial depth in the current context (working with reflected samples) and introduce an efficient approach to calculate the similarity matrix.

In order to compute the spatial depth of a point \mathbf{x} from (3), we note that it is necessary to find the vectors from all sample points to \mathbf{x} and their corresponding norms. In any of the combined dataset \mathbf{X}_{Ri} , the n points from the original dataset \mathbf{X} remain unchanged. Consequently, we can retain a $n \times d$ matrix, denoted as \mathbf{E} , to prevent redundant computations. Here, the q^{th} row is the sum of the unit vectors from other observations in \mathbf{X} to \mathbf{x}_q , expressed as:

$$\mathbf{E}_q = \sum_{\mathbf{x} \in \mathbf{X} \setminus \{\mathbf{x}_q\}} \frac{\mathbf{x}_q - \mathbf{x}}{\|\mathbf{x}_q - \mathbf{x}\|}.$$

Taking the combined dataset \mathbf{X}_{Ri} as an example, the subsequent step is to derive a similar $n \times d$ matrix $\tilde{\mathbf{E}}_i$. In this matrix, the q^{th} row is represented by

$$\tilde{\mathbf{E}}_{i,q} = \sum_{\mathbf{x} \in \mathbf{X}_{Ri} \setminus \mathbf{X}} \frac{\mathbf{x}_q - \mathbf{x}}{\|\mathbf{x}_q - \mathbf{x}\|},$$

and corresponds to the sum of the unit vectors from all the reflected points in \mathbf{X}_{Ri} to \mathbf{x}_q .

Proposition 1 (Symmetry). *Consider two distinct points \mathbf{u} and \mathbf{v} , and a point $\mathbf{x}_i \in \mathbf{X}$. Also, let \mathbf{u}^i and \mathbf{v}^i denote the points obtained by reflecting \mathbf{u} and \mathbf{v} , respectively, about \mathbf{x}_i , that is $\mathbf{u}^i = 2\mathbf{x}_i - \mathbf{u}$ and $\mathbf{v}^i = 2\mathbf{x}_i - \mathbf{v}$. Then, we have that*

$$\mathbf{u} - \mathbf{v}^i = \mathbf{v} - \mathbf{u}^i,$$

and that

$$\|\mathbf{v}^i - \mathbf{u}\|^2 = 2\|\mathbf{v} - \mathbf{x}_i\|^2 + 2\|\mathbf{u} - \mathbf{x}_i\|^2 - \|\mathbf{u} - \mathbf{v}\|^2.$$

The above result implies that we can express the squared norm of a vector from any point after reflection to an arbitrary point in \mathbf{X} , as a linear combination of the squared norms of vectors linking points in \mathbf{X} . Therefore, if the norm information is concurrently stored while generating the matrix \mathbf{E} , the norm of any vector from the reflected point to a point in \mathbf{X} can be directly computed. Let us denote the $n \times n$ square norm matrix as \mathbf{L} , where the entry in position (i, j) stores the norm of the vector between point \mathbf{x}_i and \mathbf{x}_j . This computation no longer involves calculating the root of the sum of squares of the vector coordinates, thus making the norm computation independent of the dimension d .

From Proposition 1, it can also be observed that the vector from any reflected point \mathbf{v}^i to a vector \mathbf{u} can be expressed as $\mathbf{u} + \mathbf{v} - 2\mathbf{x}_i$. Then, the sum of unit vectors from all reflection

points in \mathbf{X}_{Ri} to \mathbf{x}_q can be reformulated as follows:

$$\begin{aligned} \sum_{\mathbf{x} \in \mathbf{X}_{Ri} \setminus \mathbf{X}} \frac{\mathbf{x}_q - \mathbf{x}}{C_{\mathbf{x}}} &= \sum_{\mathbf{x} \in \mathbf{X} \setminus \{\mathbf{x}_i\}} \frac{\mathbf{x}_q + \mathbf{x} - 2\mathbf{x}_i}{C_{2\mathbf{x}_i - \mathbf{x}}} \\ &= \mathbf{x}_q \sum_{\mathbf{x} \in \mathbf{X} \setminus \{\mathbf{x}_i\}} \frac{1}{C_{2\mathbf{x}_i - \mathbf{x}}} + \sum_{\mathbf{x} \in \mathbf{X} \setminus \{\mathbf{x}_i\}} \frac{\mathbf{x} - 2\mathbf{x}_i}{C_{2\mathbf{x}_i - \mathbf{x}}}, \end{aligned}$$

where $C_{\mathbf{x}} = \|\mathbf{x}_q - \mathbf{x}\|$ and, by separating \mathbf{x}_q from the summation, we save some vector addition computations.

The matrix $\tilde{\mathbf{E}}_i$ can now be constructed using matrix computations. The necessary notations to understand this process are summarized below:

- The $(n-1) \times n$ matrix $\tilde{\mathbf{L}}_i$ stores the norms of vectors from \mathbf{x}_j^i to \mathbf{x}_q at each entry $\tilde{L}_{i,jq}$.
- The $(n-1) \times n$ matrix \mathbf{R}_i is obtained by taking the element-wise reciprocal of $\tilde{\mathbf{L}}_i$, i.e., $R_{i,jq} = 1/\tilde{L}_{i,jq}$.
- The $(n-1) \times d$ matrix $\tilde{\mathbf{X}}_i$ contains each reflected point (excluding \mathbf{x}_i itself) as a row.
- The $n \times d$ matrix \mathbf{B}_i consists of points in \mathbf{X} , each multiplied by the corresponding column sum of \mathbf{R}_i .

With these, $\tilde{\mathbf{E}}_i$ is expressed as: $\tilde{\mathbf{E}}_i = \mathbf{B}_i - \mathbf{R}_i' \tilde{\mathbf{X}}_i$. Through the above procedure, $\tilde{\mathbf{E}}_i$ can be derived efficiently. For instance, in a 2000×600 dataset, while \mathbf{E} requires approximately two seconds to compute, $\tilde{\mathbf{E}}_i$ only takes around 0.1 second per loop — run on a PC with Intel(R) Core(TM) i7-11700K processor (3.6 GHz) with sufficiently large physical memory, Matlab R2023a. Having obtained \mathbf{E} and $\tilde{\mathbf{E}}$, the reflection spatial depth values of any \mathbf{x}_q in \mathbf{X} based on \mathbf{X}_{Ri} can be computed via

$$D_{SD}(\mathbf{x}_q | \mathbf{X}_{Ri}) = 1 - \left\| \frac{\mathbf{E}_q + \tilde{\mathbf{E}}_{i,q}}{2n-1} \right\|. \quad (7)$$

III. DEPTH-BASED LOCAL CENTER CLUSTERING

In this section, we first introduce some concepts that are key to DLCC and then provide a detailed explanation of the clustering procedure.

As explained in Section II, it is necessary to use an appropriately localized version of data depth for clustering applications. In the framework of DLCC, we establish two foundational concepts: neighborhoods and local ranks. These concepts are formalized in the following definition:

Definition 1 (DLCC Neighborhoods and Local Ranks). ***Neighbors and Neighborhoods:** Given an integer parameter s , the neighbors of $\mathbf{x}_i \in \mathbf{X}$ are defined as the set of $s-1$ points $\mathbf{x}_q \in \mathbf{X} \setminus \{\mathbf{x}_i\}$ with the highest depth values with respect to the dataset \mathbf{X}_{Ri} , i.e., the points with the largest $D(\mathbf{x}_q | \mathbf{X}_{Ri})$. The neighborhood of \mathbf{x}_i , denoted as \mathbf{N}_i , is thus formed by including \mathbf{x}_i and its $s-1$ neighbors, constituting a subset of \mathbf{X} with size s .*

***Local Depth [37] and Local Ranks:** The local depth of an observation \mathbf{x}_i is its depth value within its neighborhood \mathbf{N}_i . The local rank of an observation \mathbf{x}_j within the neighborhood \mathbf{N}_i is defined as:*

$$r_i(\mathbf{x}_j) = 1 + \sum_{\mathbf{x}_q \in \mathbf{N}_i} \mathbb{I}[D(\mathbf{x}_j | \mathbf{N}_i) < D(\mathbf{x}_q | \mathbf{N}_i)], \quad (8)$$

where \mathbb{I} denotes the indicator function.

If $r_i(\mathbf{x}_j) = 1$, then \mathbf{x}_j is characterized as the center of the subset \mathbf{N}_i . We define central points of \mathbf{N}_i as a local center. These local centers can be understood as representative points for the entire dataset \mathbf{X} .

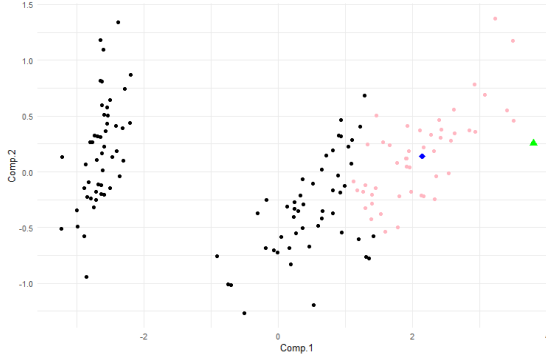


Fig. 3: Local center example ($s = 50$) for the first two PCs of the Iris dataset, where a focus point (green triangle) with its neighbors (pink points) and the corresponding local center (blue diamond) are highlighted.

Notes:

- 1) While \mathbf{x}_i is deepest in \mathbf{X}_{R_i} by construction, it is not generally deepest in \mathbf{N}_i , as illustrated in Figure 3.
- 2) There should be less than n unique local centers due to the occurrence of shared local centers among the sets \mathbf{N}_i . The frequency of a local center, denoted by f , is defined as the number of neighborhoods that share this local center.

The DLCC method uncovers clusters through analyzing and grouping local centers. However, as n subsets might yield a large number of local centers, many of them might not be useful for clustering. For example, an outlier residing between two clusters can be the deepest point in a subset containing observations from both clusters. Hence, it is crucial to filter out unnecessary local centers before grouping them. The remaining centers after filtering are denoted as filtered centers.

DLCC introduces two strategies designed to address diverse types of clustering challenges. The conditions for grouping the filtered centers under these two strategies are summarized as follows:

Definition 2. Let c_1, \dots, c_A denote a finite set of filtered centers and $\mathbf{N}_{c_1}, \dots, \mathbf{N}_{c_A}$ their corresponding neighborhoods. Define the similarity between any two neighborhoods as the proportion of overlapping observations among them. Two grouping strategies are as follows:

- **Min strategy:** for any $c \in \mathbf{g}_i$:

$$\min_{c^* \in \mathbf{g}_i} \text{sim}(\mathbf{N}_c, \mathbf{N}_{c^*}) > \max_{j \neq i} \min_{c^\dagger \in \mathbf{g}_j} \text{sim}(\mathbf{N}_c, \mathbf{N}_{c^\dagger}) \quad (9)$$

$$\max_{c^* \in \mathbf{g}_i \setminus \{c\}} \text{sim}(\mathbf{N}_c, \mathbf{N}_{c^*}) > \max_{c^\dagger \notin \mathbf{g}_i} \text{sim}(\mathbf{N}_c, \mathbf{N}_{c^\dagger}). \quad (10)$$

- **Max strategy:** Given a parameter δ , termed as the similarity threshold, $\forall c$ in group \mathbf{g} , $\exists c^*$ in the same group s.t. $\text{sim}(\mathbf{N}_c, \mathbf{N}_{c^*}) > \delta$, and for $\forall c^\dagger \notin \mathbf{g}$, $\text{sim}(\mathbf{N}_c, \mathbf{N}_{c^\dagger}) \leq \delta$.

Note that, “group” refers specifically to a set of filtered centers and should not be confused with “cluster”. Some insights into the strategy chosen for grouping local centers are important in applications. Under the min strategy, DLCC attempts to find centroids of clusters from filtered centers. The variance in the number of filtered centers across different groups allows for better flexibility than traditional center-based clustering methods, especially when dealing with clustering problems that have overlapping regions. The min strategy tends to be more suitable when the sizes of all clusters are comparable.

The max strategy assumes each cluster can be built by connecting multiple finite convex shapes created by filtered centers. Filtered centers in the same group are connected with a chain of similarities. For example, if two filtered centers c_y and c_z are in the same group, then there must exist a chain of filtered centers, $c_{p_1}, c_{p_2}, \dots, c_{p_h}$, where $c_{p_1} = c_y$, $c_{p_h} = c_z$, and the similarity between any two adjacent centers’ neighborhoods in that chain is larger than δ . Generally, the parameter s is small under the max strategy. When using Mahalanobis depth to construct the similarity matrix with a small s , the max strategy is less sensitive to variations in the matrix. In such cases, a globally estimated similarity matrix often suffices, similar to DBCA. However, unlike DBCA, which builds clusters with chains of fixed-shape ellipses centered at each observation, DLCC with the max strategy considers only chains of filtered centers, with a fixed number of neighbors rather than a fixed region. Like density-based methods, the max strategy works well for disjoint clusters and can handle non-convex clusters of varying sizes.

Definition 3 (Unique neighbor). Define $\bigcup_{c_i \in \mathbf{g}} \mathbf{N}_{c_i}$ and $\bigcup_{c_j \notin \mathbf{g}} \mathbf{N}_{c_j}$ as the unions of neighborhoods for filtered centers within and outside of group \mathbf{g} , respectively. The set of unique neighbors for \mathbf{g} , $\mathbf{U}_{\mathbf{g}}$, is the largest subset of $\bigcup_{c_i \in \mathbf{g}} \mathbf{N}_{c_i}$ satisfying:

$$\mathbf{U}_{\mathbf{g}} \cap \bigcup_{c_j \notin \mathbf{g}} \mathbf{N}_{c_j} = \emptyset.$$

The number of clusters, denoted by K , aligns with the grouping of the filtered centers. Temporary clusters are derived from the unique neighbors of each group. The details of constructing these temporary clusters based on the unique neighbors and filtered centers will be further elaborated later in this section.

With these temporary clusters, it is expected that most observations have been allocated to a particular cluster. Nevertheless, there may still be some points that remain unclustered. In such cases, the clustering problem can be reframed as a classification problem. Intuitively, classification methods can be used to assign the remaining points to a cluster. It should be noted that the choice of classification method is very flexible here. Indeed, we could potentially consider any classification method at this stage, depending on the specific requirements of the task at hand. DLCC incorporates three built-in classification methods: maximum-depth classifier (MDC), K-nearest neighbors (KNN) based on the similarity matrix, and random forests (RF).

Lastly, self-improvement procedures of DLCC are dis-

cussed. Although the clustering problem is converted to a classification problem in the final stage, it has some special features, because the observations that are already labelled may still be updated. Two logical parameters are introduced here:

- **maxdepth**: This parameter dictates whether DLCC will continue iterations until all observations in the assigned cluster attain the highest depth values.
- **ifloop**: This parameter, only applicable under the min strategy, determines whether only a single filtered center should remain in each cluster.

Let the K clusters constructed so far be denoted by \mathcal{X}_k , where $k = 1, 2, \dots, K$. For any observation \mathbf{x}_j , $D(\mathbf{x}_j | \mathcal{X}_k)$ corresponds to the depth of this observation within cluster \mathcal{X}_k . If the depth value of \mathbf{x}_j in the cluster it is currently assigned to does not match $\max_k D(\mathbf{x}_j | \mathcal{X}_k)$, and if the “maxdepth” parameter is set to TRUE, \mathbf{x}_j will be relocated. This procedure loops until all observations are assigned to the cluster where they obtain the largest depth value. Regarding the min strategy, it can be adapted to resemble a centroid-based clustering method. If the “ifloop” parameter is TRUE, the clustering algorithm updates clusters using only the deepest filtered center within each cluster. However, other filtered centers are not disregarded. They may become the deepest center for a cluster in future iterations, as clustering results are reassessed after each update. This iterative process continues, regenerating clusters and potentially re-evaluating the roles of filtered centers, until the clustering outcome stabilizes.

A. Local Center Selection and Grouping

Locating and filtering local centers is at the core of DLCC. For neighborhoods $\mathbf{N}_1, \mathbf{N}_2, \dots, \mathbf{N}_n$ of size s , local centers are identified. To filter local centers, two benchmarks are suggested:

- a local center should be central to its neighborhood; and
- a local center with higher frequency f is more reliable.

The first step of filtering local centers is to pick up local centers satisfying $r_i(\mathbf{x}_i) \leq 2$ (Definition 1), which aims to meet the first benchmark. The requirement of a central position is relaxed from $r_i(\mathbf{x}_i) = 1$ to $r_i(\mathbf{x}_i) \leq 2$ for adding flexibility. Local centers with $f = 1$ are discarded next, as they are less reliable. The remaining steps in filtering local centers differ between the min and max strategies.

1) *Min strategy*: After the first filtering step, assume there are T local centers remaining. Index these local centers in the decreasing order of their frequencies, i.e., $\{c_1, \dots, c_T\}$, which corresponds to $f_1 \geq f_2 \geq \dots \geq f_T$. With this order, the cumulative proportion of neighbors for the local centers down the list can be calculated as

$$\mathcal{P}_t = \frac{1}{n} \left| \bigcup_{p=1}^t \mathbf{N}_{c_p} \right|, \quad (11)$$

where $|\cdot|$ represents the cardinality of a set.

The filtering procedure consists of two steps: (1) selecting a suitable frequency cutoff, and (2) adjusting the grouping results to satisfy the min strategy defined in Definition 2.

According to Definition 2, for fixed local centers, the grouping result satisfying the max strategy is unique, whereas multiple solutions may satisfy the min strategy. Thus, a reasonable initial grouping method that provides high-quality results and estimates the number of groups is essential. We summarize the designed grouping method in Algorithm 1. This method leverages local depths and the similarities between neighborhoods of local centers. Here, local depth values are computed during defining local centers, and the similarity matrix for neighborhoods of local centers is denoted as \mathbb{M} , with $\text{sim}(\mathbf{N}_{c_i}, \mathbf{N}_{c_j})$ as its ij -th entry.

Algorithm 1 Local depth and similarity-based grouping

Input: Local centers c_1, \dots, c_T , corresponding top $s/2$ neighbors, local depth values (LD), similarity matrix \mathbb{M} , and a similarity threshold range $[0.4, 0.75]$.

Output: Grouping results $\{\mathbf{g}_1, \mathbf{g}_2, \dots, \mathbf{g}_G\}$.

- 1: For each local center c_i , set valid neighbors VN_i as local centers in its top $s/2$ neighbors (excluding itself).
- 2: Initialize mean similarities and closest neighbors: $\text{MS} =$ zero array of size T , $\text{CN} = 1:T$
- 3: **for** $t = 1$ to T **do**
- 4: Compute mean similarity: $\text{MS}_t = \frac{\sum_{c_j \in \text{VN}_t} \mathbb{M}_{tj}}{|\text{VN}_t|}$.
- 5: Find the closest neighbor: $\text{CN}_t = \arg \max_{j \neq t} \mathbb{M}_{tj}$.
- 6: **end for**
- 7: Set similarity threshold δ_i for each local center c_i :

$$\delta_i = \min(\text{MS}_i, \text{MS}_{\text{CN}_i})$$

and if $\delta_i \notin [0.4, 0.75]$ adjust it to the nearest bound.

- 8: Initialize stable centers $\text{SC} = \emptyset$.
 - 9: **for** $t = 1$ to T **do**
 - 10: **if** All $c_j \in \text{VN}_t$ with $\text{sim}(\mathbf{N}_{c_t}, \mathbf{N}_{c_j}) \geq \delta_t$ have $\text{LD}_j < \text{LD}_t$ **then**
 - 11: Add c_t to SC .
 - 12: **end if**
 - 13: **end for**
 - 14: Set $G = |\text{SC}|$.
 - 15: Assign each remaining local center to the group of its most similar stable center using \mathbb{M} .
 - 16: Return groups $\{\mathbf{g}_1, \mathbf{g}_2, \dots, \mathbf{g}_G\}$.
-

Algorithm 1 uses local depth to assess the centrality of each center and employs neighborhood similarity to evaluate the relationship between centers. The similarity threshold is determined automatically, eliminating the need for manual parameter selection. Specifically, the threshold for each center c is set as the minimum of the mean similarity between c and its closest neighbor. This approach provides a center-specific threshold while ensuring that centers with similar neighborhoods share comparable thresholds. The empirical threshold range $[0.4, 0.75]$ prevents the values from being excessively small or large. Moreover, the algorithm naturally estimates the number of groups, which corresponds to the number of estimated clusters.

A limitation of Algorithm 1 is if multiple clusters overlap with each other, the local center defined in the overlapped region may have high local depth values. These local centers

can be removed by analyzing the number of unique neighbors (Definition 3) within each group, as groups containing local centers from overlapped regions tend to have very few unique neighbors. Specifically, we consider a group of centers should be dropped if the number of unique neighbors of this group is less than $s/10$. Additionally, local centers highly similar to those in the identified group should also be dropped to avoid ambiguity.

With the grouping of local centers, we determine candidates for the cutoff in the order of frequency. The first candidate index is defined as

$$\max \left(\arg \min_t \{ \mathcal{P}_t \geq 0.75 \}, \max_{\mathbf{g}} \{ \arg \min_{t: c_t \in \mathbf{g}} t \} \right), \quad (12)$$

where the first term ensures the final cumulative proportion \mathcal{P}_t exceeds 0.75 to prevent excessive elimination of local centers, and the second term guarantees at least one local center from each group is retained.

Additional candidates include local centers after the begin index that provide complementary information beyond those in the same group with higher frequency. Specifically, a candidate index i must satisfy two conditions: First for all c_j where $j \leq i$ and c_j belongs to the same group \mathbf{g} as c_i ,

$$\sum_j \mathbb{M}_{ij} = \min_{l \leq i, c_l \in \mathbf{g}} \sum_j \mathbb{M}_{lj}, \quad (13)$$

This ensures c_i is the least similar to other local centers with higher frequencies in its group. Second, for all c_v where $v < i$ and $c_v \notin \mathbf{g}$,

$$\max_v \mathbb{M}_{iv} \leq \min_{j < i, c_j \in \mathbf{g}} \max_v \mathbb{M}_{jv}, \quad (14)$$

ensuring c_i is less similar to points in other groups compared to any existing local center in its own group. In essence, these candidates are distant from local centers in other groups while also comparatively distinct within their own group, making them potential sources of complementary information.

Lastly, we evaluate each candidate in ascending order and count the number of ‘‘bad points’’ between candidates, defined as local centers that fail to satisfy Equations (9) or (10) after removing local centers in groups with indices larger than the candidate. If the number of bad points between two consecutive candidates c_i and $c_{i'}$ exceeds 1, we stop at c_i .

In the above setting, the initial candidate should have a cumulative proportion of at least 0.75. However, if $\mathcal{P}_T < 0.75$, it may indicate that overlapping clusters cause local centers to concentrate in shared regions rather than capturing true subcluster centers. The robustness of the depth median (e.g. SD’s breakdown point is 0.5) biases local centers toward overlapping regions when most points in a cluster have neighborhoods with similarities exceeding 0.5 to points in other clusters. To address this, if $\mathcal{P}_T < 0.75$, we retain only centers dissimilar to those in other groups after grouping c_1, \dots, c_T using Algorithm 1. For $c \in \mathbf{g}$, we check:

$$\frac{\sum_{j: c_j \in \mathbf{g} \setminus c_i} \mathbb{M}_{ij}}{|\mathbf{g}| - 1} - \max_{v: c_v \notin \mathbf{g}} \mathbb{M}_{iv} > 0. \quad (15)$$

Then, we iteratively add back local centers from the dropped

ones, including those with $f = 1$ or $r_i(\mathbf{x}_i) > 2$. In each step, the local center that maximizes the increase in cumulative proportion is added back. The process stops when the cumulative proportion exceeds 90% of the cumulative proportion of all local centers.

Algorithm 2 Local center filtering under the min strategy

Input: All local centers, their ranks, frequencies, local depth values, neighborhoods, size s and similarity matrix \mathbb{M} .

Output: Filtered local centers and their local depth values.

- 1: Perform initial filtering to obtain $\{c_1, \dots, c_T\}$.
- 2: **if** $\mathcal{P}_T \geq 0.75$ **then**
- 3: Apply Algorithm 1 to obtain $\{\mathbf{g}_1, \dots, \mathbf{g}_G\}$.
- 4: Set Continue as True.
- 5: **while** Continue **do**
- 6: Obtain unique neighbors $\{\mathbf{U}_{\mathbf{g}_1}, \dots, \mathbf{U}_{\mathbf{g}_G}\}$.
- 7: Identify $d_i = \arg \min_{i: |\mathbf{U}_{\mathbf{g}_i}| < s/10} |\mathbf{U}_{\mathbf{g}_i}|$.
- 8: **if** $d_i \neq \emptyset$ **then**
- 9: Set $\delta = \max_{i, j \in \mathbf{g}_{d_i}, i \neq j} \mathbb{M}_{ij}$.
- 10: Mark centers in \mathbf{g}_{d_i} as drop centers.
- 11: Add centers v outside \mathbf{g}_{d_i} to drop centers if $\max_{i: c_i \in \mathbf{g}_{d_i}} \mathbb{M}_{vi} \geq \delta$.
- 12: Remove \mathbf{g}_{d_i} and drop centers, and update G .
- 13: **else**
- 14: Set Continue as False;
- 15: **end if**
- 16: **end while**
- 17: Define the first cutoff candidate cc_1 as in (12).
- 18: Identify additional candidates among centers with indices greater than cc_1 and satisfy (13) and (14).
- 19: Initialize bp = zero array of size $|cc|$.
- 20: **for** $q = 1$ to $|cc|$ **do**
- 21: Remove local centers in groups with indices larger than cc_q to form $\{\mathbf{g}'_1, \dots, \mathbf{g}'_G\}$.
- 22: Compute $bp_q = |c \text{ violates (9) or (10)}|$ for all $c \in \{\mathbf{g}'_1, \dots, \mathbf{g}'_G\}$.
- 23: **end for**
- 24: Define cutoff as cc_p where p is the first index satisfying $bp_{p+1} - bp_p > 1$. If no such p exists, set cc_p as the largest cutoff candidate index.
- 25: **else**
- 26: Drop local centers from $\{c_1, \dots, c_T\}$ that do not satisfy (15).
- 27: Compute current cumulative proportion \mathcal{P} and total cumulative proportion \mathcal{P}' .
- 28: **while** $\mathcal{P} < 0.9\mathcal{P}'$ **do**
- 29: Add the local center maximizes the increase in \mathcal{P} .
- 30: Update \mathcal{P} .
- 31: **end while**
- 32: **end if**
- 33: Save remaining local centers and their local depth values.

After Algorithm 2, we reapply Algorithm 1 to group the filtered centers. If any local centers fail to meet the requirements of the min strategy, Algorithm 3 is applied, which is referred to as the group trimming process. The number of clusters is not required, but if users specify K , the algorithm forces the number of groups to equal K . For simplicity, the left and right

Algorithm 3 Group Trimming Process

Input: Groups of local centers $\{\mathbf{g}_1, \dots, \mathbf{g}_G\}$, similarity matrix \mathbb{M} , optional K .

Output: Trimmed groups satisfying the min strategy.

```

1: if  $K \neq \emptyset$  then
2:   if  $G > K$  then
3:     Drop groups with the highest  $\{\arg \min_{t: c_t \in \mathbf{g}} t\}$ 
     until  $G$  equals to  $K$ .
4:   else
5:     while  $G < K$  do
6:       Define a new stable center and increment  $G$  by
7:       1.  $\triangleright$  Details provided in supplementary material
8:     end while
9:     Update  $\{\mathbf{g}_1, \dots, \mathbf{g}_G\}$ .
10:  end if
11: while violations of (9) or (10) exist do
12:   while violations of (9) exist do
13:    for each group  $\mathbf{g}_l$  with violations of (9) do
14:      Drop the center  $c \in \mathbf{g}_l$  which maximizes:
      
$$\frac{\sum_{c' \in \mathbf{g}_l \setminus \{c\}} (\text{mw}(c') - \text{mb}(c'))}{|\mathbf{g}_l \setminus \{c\}|}$$

15:    end for
16:    Update groups and recompute violations of (9).
17:   end while
18:   if violations of (10) exist then
19:     Drop all centers violating (10).
20:     Update groups and recompute violations.
21:   end if
22: end while

```

sides of inequality (9) are denoted as $\text{mw}(c)$ and $\text{mb}(c)$ in the algorithm, respectively.

2) *Max strategy:*

Definition 4 (Isolated Local Center). *A local center c_i is considered isolated if, for all $c_j \neq c_i$, the similarity between the neighborhoods associated with c_i and c_j is zero, i.e.,*

$$\mathbb{M}_{ij} = 0.$$

In other words, an isolated local center is one whose neighborhood does not overlap with any other neighborhoods. As the max strategy assumes each cluster consists of various convex shapes, if there are any isolated local centers, they will be discarded.

Definition 5 (Everywhere Non-Convex Cluster). *An everywhere non-convex cluster is characterized by all of its points having non-convex neighborhoods. Examples include one-dimensional manifolds, such as spirals, and self-crossing curves. A region containing such a cluster is termed a locally non-convex region.*

The max strategy fails to identify everywhere non-convex clusters because as the depth functions used herein only suit convex shapes, preventing recognition of local centers satisfying $r_i(\mathbf{x}_i) \leq 2$ in a non-convex neighborhood. To assess

Algorithm 4 Segregating the locally non-convex region

Input: Sets of local centers \mathbf{c}_1 , \mathbf{c}_2 , and \mathbf{c}_3 , neighborhood similarity matrix \mathbb{M}

Output: Set of filtered centers \mathbf{C}

```

1: if  $\mathbf{c}_2 \neq \emptyset$  then
2:   for  $v$  in the indices of local centers in  $\mathbf{c}_3$  do
3:     if  $\max_{j: c_j \in \mathbf{c}_2} \mathbb{M}_{vj} > \max_{i: c_i \in \mathbf{c}_1} \mathbb{M}_{vi}$  then
4:        $\mathbf{c}_2 = \mathbf{c}_2 \cup \{c_v\}$ 
5:       for  $i$  in the indices of local centers in  $\mathbf{c}_1$  do
6:         if  $\mathbb{M}_{vi} > 0$  then
7:            $\mathbf{c}_1 = \mathbf{c}_1 \setminus \{c_i\}$ 
8:         end if
9:       end for
10:     end if
11:   end for
12:    $\mathbf{C} = \mathbf{c}_1 \cup \mathbf{c}_2$ 
13:   if any isolated local centers exist based on  $\mathbf{C}$  then
14:     Remove isolated local centers from  $\mathbf{C}$ 
15:   end if
16: else
17:    $\mathbf{C} = \mathbf{c}_1$ 
18: end if

```

the presence of everywhere non-convex clusters and mitigate their impact, we categorize local centers into three sets based on the outcome of prior filtering:

- Set \mathbf{c}_1 includes all local centers that remain after initial filtering, characterized by non-isolated local centers with $r_i(\mathbf{x}_i) \leq 2$ and $f \neq 1$.
- Set \mathbf{c}_2 contains non-isolated local centers c_v for which $\forall c_i \in \mathbf{c}_1$, c_v satisfies $\mathbb{M}_{vi} = 0$.
- Set \mathbf{c}_3 consists of local centers $c_v \notin \mathbf{c}_1$ satisfying $\exists c_i \in \mathbf{c}_1$ such that $\mathbb{M}_{vi} > 0$.

The presence of everywhere non-convex clusters is inferred if \mathbf{c}_2 is not empty. In such cases, Algorithm 4 are taken to segregate locally non-convex regions from other clusters.

Algorithm 4 ensures that local centers in \mathbf{c}_2 , which capture the essence of locally non-convex regions, remain disjoint with the local centers in other clusters, i.e., local centers in \mathbf{c}_1 .

B. Clustering in DLCC

Assuming the grouping results for the filtered centers are at hand, with the unique neighbors of each group serving to initialize temporary clusters, let \mathbf{C} represent the set of filtered centers, such that $\mathbf{C} = \bigcup_{k=1}^G \mathbf{g}_k$, where G denotes the total number of groups, and \mathbf{g}_k contains the filtered centers of the k th group. Consequently, the number of clusters K is inherently defined to be equal to G , as each group's unique neighbors directly initiate a corresponding temporary cluster. The subsequent step involves defining a score for each observation with respect to each cluster in order to update these temporary clusters.

1) *Min strategy:* For the min strategy, the score accounts for both clustering and assessing if each observation's clustering result is acceptable, and it is computed using the similarity matrix \mathbb{S} . If \mathbb{S} is asymmetric, it is updated by replacing \mathbb{S}_{ji}

and \mathbb{S}_{ij} with their average value. For clarity, we continue to denote the symmetrized matrix as \mathbb{S} , ensuring that $\mathbb{S}_{ij} = \mathbb{S}_{ji}$ in this and the subsequent discussion about the DC metric in Section IV. We define the score function for an observation \mathbf{x}_i with respect to a temporary cluster k under the min strategy as

$$\text{score}_{i|k} = \frac{\max_{j \in \mathcal{I}_k} \mathbb{S}_{ji} - \max_{j \in \bigcup_{z \neq k} \mathcal{I}_z} \mathbb{S}_{ji}}{\max\{\max_{j \in \mathcal{I}_k} \mathbb{S}_{ji}, \max_{j \in \bigcup_{z \neq k} \mathcal{I}_z} \mathbb{S}_{ji}\}}, \quad (16)$$

where \mathcal{I}_k is the set of indices for filtered centers within the k th group, i.e., $\mathcal{I}_k = \{j : \mathbf{x}_j \in \mathbf{g}_k\}$. The score (16) takes a value between -1 and 1 and a positive value indicates that, compared with the nearest filtered center in other groups, the similarity between \mathbf{x}_i and the nearest filtered center in group k is larger.

For each cluster, two score pools are generated: \mathcal{S}_k , containing both the unique neighbors within the cluster ($\mathbf{U}_{\mathbf{g}_k}$) and their corresponding scores, and $\hat{\mathcal{S}}_k$, holding observations not in $\mathbf{U}_{\mathbf{g}_k}$ yet having positive scores toward this cluster, along with their scores. Upon reviewing these pools, observations with high scores may shift from $\hat{\mathcal{S}}_k$ to \mathcal{S}_k , and vice versa, for those with low scores in \mathcal{S}_k . Lastly, \mathcal{S}_k includes observations confidently assigned to the cluster, while those in $\hat{\mathcal{S}}_k$ remain unlabelled. Note that during the reassignment of observations between pools, their corresponding scores are also moved. The detailed steps are outlined as Algorithm 5, where the second element of the min function in line 14 ensures at least $s/2$ observations per temporary cluster, preventing overly small clusters. Figure 4 illustrates an example using the Yale B face recognition dataset [56]. Algorithm 5 removes labels from unique neighbors within each group that are less distinguishable from other points in their own group. Meanwhile, it assigns labels to points that are not unique neighbors but are relatively closer to the filtered centers of their group.

2) *Max strategy*: The score for the max strategy is only for overlapping neighbors between filtered centers in different groups, and is defined as

$$\text{score}_{e_i|k} = \frac{|\{c \in \mathbf{g}_k \mid \mathbf{x}_i \in \mathbf{N}_c\}|}{|\mathbf{g}_k|}. \quad (17)$$

Observations that are neighbors of filtered centers in different groups are allocated to the cluster with the highest score. Unlabeled observations either do not have the highest unique score or are not neighbours of any filtered center.

3) *Classification*: Among three built-in classification methods for the remaining unlabelled observations, MDC is the non-parametric method based on data depth. MDC assigns each observation to the cluster within which it achieves its maximum depth value. To ensure consistency in our methodology, we employ the same type of data depth in the MDC as we used in defining the local centers. When Mahalanobis depth is chosen, the covariance matrix in the classification step is estimated using traditional moment estimation methods. This is based on the theoretical consideration that temporary clusters are subsets of clusters and all observations in these temporary clusters are selected with a degree of confidence.

As for the KNN method, it is an intuitive classification method and is suitable for non-convex shapes. Given that we

Algorithm 5 Update Temporary Cluster

Input: Score pools \mathcal{S}_k and $\hat{\mathcal{S}}_k$ for $k = 1, \dots, K$, where \mathcal{S}_k^1 and $\hat{\mathcal{S}}_k^1$ represent observations, and \mathcal{S}_k^2 and $\hat{\mathcal{S}}_k^2$ represent the corresponding scores, neighborhood size s .

Output: Updated score pool \mathcal{S}_k , where \mathcal{S}_k^1 constructs the k -th temporary cluster.

```

1: for  $k = 1$  to  $K$  do
2:    $\gamma_1 = \text{mean}(\hat{\mathcal{S}}_k^2)$ 
3:   for  $i$  in  $\mathcal{S}_k^2$  do
4:     if  $i < \gamma_1$  then
5:        $\mathcal{S}_k^2 = \mathcal{S}_k^2 \setminus \{i\}$ 
6:        $\hat{\mathcal{S}}_k^2 = \hat{\mathcal{S}}_k^2 \cup \{i\}$ 
7:       Move corresponding points from  $\mathcal{S}_k^1$  to  $\hat{\mathcal{S}}_k^1$ 
8:     end if
9:   end for
10:   $SS = \text{Sort scores in } \mathcal{S}_k^2 \text{ in descending order}$ 
11:   $B = \text{length of } SS$ 
12:   $idx = \arg \max_{j=\text{floor}(B/2) \text{ to } B-1} (SS[j] - SS[j+1])$ 
13:   $\hat{B} = \text{length of } \hat{\mathcal{S}}_k^2$ 
14:   $\gamma_2 = \min(SS[idx], 1 - \frac{s/2-B}{\hat{B}} \text{quantile of } \hat{\mathcal{S}}_k^2)$ 
15:  for  $u$  in  $\hat{\mathcal{S}}_k^2$  do
16:    if  $u > \gamma_2$  then
17:       $\hat{\mathcal{S}}_k^2 = \hat{\mathcal{S}}_k^2 \setminus \{u\}$ 
18:       $\mathcal{S}_k^2 = \mathcal{S}_k^2 \cup \{u\}$ 
19:      Move corresponding points from  $\hat{\mathcal{S}}_k^1$  to  $\mathcal{S}_k^1$ 
20:    end if
21:  end for
22: end for

```

have already constructed the similarity matrix \mathbb{S} , the KNN method in our algorithm identifies neighbors through depth-based similarity, rather than relying on Euclidean distance. As such, the method identifies neighbors directly within \mathbb{S} , thus eliminating the need for additional computational steps.

The last method, RF, is a renowned machine learning algorithm and has a wide range of applications. In classification, it operates without assumptions on the shapes of the clusters and can demonstrate satisfactory performance even in high-dimensional spaces.

IV. EXPLORING PARAMETER SELECTIONS

The choice of parameters s (neighborhood size) and δ (neighborhood similarity threshold) affect the resulting clustering differently. The neighborhood size s directly affects the defined neighborhoods for each observation and hence impacts the construction of the set \mathbf{C} of filtered centers. Under the max strategy, for any given s , the value of δ further influences how the filtered centers are grouped. Basically, a smaller value of δ results in fewer, and larger, groups of filtered centers.

A. Hierarchical Structure of grouping under the max strategy

Under the max strategy, given a certain s , all possible values of the number of groups can be derived. By starting at $\delta = \delta_0$ and progressively reducing δ , all δ 's at the time that the number of groups changes can be recorded.

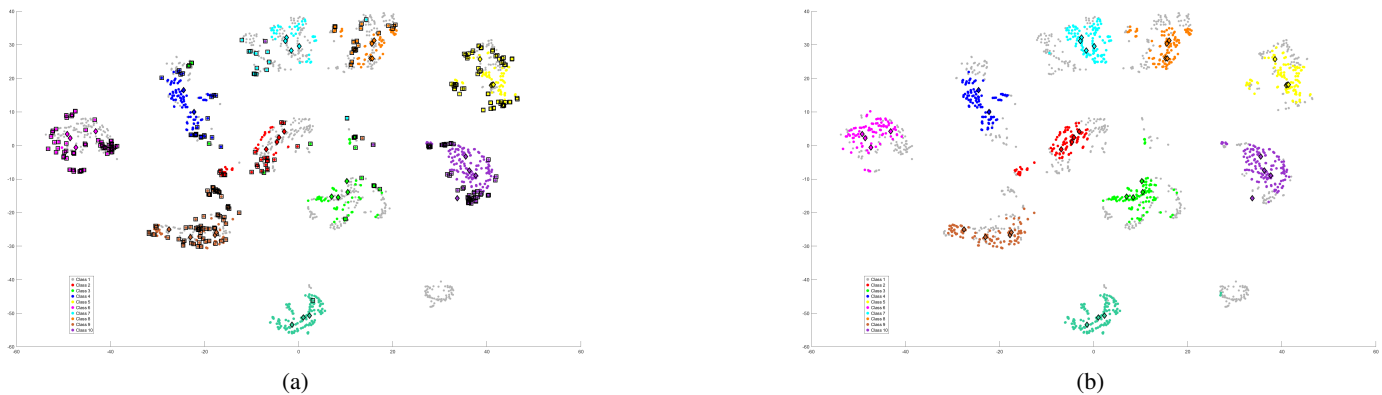


Fig. 4: t-SNE visualization [47] of the Yale B dataset. Colors represent the true labels of the points, with only those in temporary clusters being colored. Points enclosed by diamond-shaped boxes represent filtered centers. (a) Initial points in \mathcal{S}_k , with points enclosed by square boxes indicating those to be moved to $\hat{\mathcal{S}}_k$. (b) The temporary clusters obtained after applying Algorithm 5.

The initial choice for δ can be based on the following value:

$$\delta_U := \min_c \max_{c^\dagger} \{\text{sim}(\mathbf{N}_c, \mathbf{N}_{c^\dagger}) : c \neq c^\dagger \in \mathbf{C}\}. \quad (18)$$

For any $\delta \geq \delta_U$, there will be at least one group with a single filtered center. It is thus desirable to start with a smaller value, say $\delta_0 = 0.99\delta_U$, so that multiple smaller subsets are connected to form clusters.

Suppose δ_0 is chosen, partitioning \mathbf{C} into groups $\mathbf{g}_1, \mathbf{g}_2, \dots$. Now, if we reduce the δ value from δ_0 to a value below the maximum similarity among neighborhoods of centers between any two groups \mathbf{g}_i and \mathbf{g}_j , as described by:

$$\delta < \max\{\text{sim}(\mathbf{N}_c, \mathbf{N}_{c^\dagger}) : c \in \mathbf{g}_i, c^\dagger \in \mathbf{g}_j\}, \quad (19)$$

then \mathbf{g}_i and \mathbf{g}_j will merge. The value in (19) is referred to as the grouping critical point for \mathbf{g}_i and \mathbf{g}_j . Observing how grouping results evolve as δ decreases from δ_0 reveals the hierarchical clustering structure. We use a toy example to illustrate the process, shown in Figure 5. Each square matrix is referred to as a “grouping matrix”. The order of the matrix denotes the number of groups, and its entries identify the grouping critical points among these groups for a given δ value. In each step, the grouping matrix obtained from the previous one by merging columns and rows that contain the largest non-trivial (not 0 or 1) value. The merging process retains the larger of the values in the corresponding entries of the columns and rows. Eventually, we are left with completely disjoint groups, represented by the identity matrix as the grouping matrix.

The process of grouping generates two key lists: one for the number of groups and another for the corresponding threshold values. More precisely, in the toy example, the potential numbers of groups are 6, 4, 3, and 2, with the δ values ranging between the intervals $[0.6, \delta_U)$, $[0.5, 0.6)$, $[0.4, 0.5)$, and $[0, 0.4)$ at each stage. The hierarchical structure ensures that if the number of clusters is known or can be estimated using any methods (refer to [48] for estimation techniques), a suitable δ can be directly determined from the relationship between the lists \mathbf{G} and δ .

B. Depth-Based Clustering Metric

The next challenge of parameter selection is to identify the optimal pair of parameters (s, δ) , which requires an appropriate internal metric to determine the best clustering among various results. However, the DLCC under the max strategy often addresses clustering problems involving non-convex shapes or closely positioned clusters of significantly different sizes, where well-known internal metrics such as ASW and CHI encounter difficulties. The limitations of these metrics are illustrated using two synthetic datasets, SmileyF and Bainba — see Figures 1 and 6, and Table II. In both figures, the clustering results in (a) are the actual labels for the datasets, for which both ASW and CHI yield low scores. Both criteria awarded high scores to the clustering result (c) in the SmileyF dataset, although human assessment considers (c) to perform the poorest. Similarly, both criteria favour clustering result (b) for the Bainba dataset, which contains only two clusters. This discrepancy highlights the need for a metric that better handles clustering of complex shapes.

TABLE II: ASW and CHI values corresponding to the clustering results in Figures 6 and 1.

	Label	(a)	(b)	(c)
Bainba: ASW		0.341	0.491	0.339
Bainba: CHI		642.13	842.52	641.99
SmileyF: ASW		-0.146	-0.152	0.435
SmileyF: CHI		45.25	43.18	1470.62

The DC metric is introduced to evaluate and compare different clustering outcomes when the ground truth is not available, facilitating the identification of the optimal pair of parameters. The main idea is to calculate within- and between-cluster similarities in a small, fixed region instead of computing similarities globally to handle non-convex clusters. This approach, inspired by the DBCA methodology [33], is adapted in our context with a broader scope. While DBCA specifies similarity as $D_{\text{MD}}^i(\mathbf{z})$, we generalize this concept to

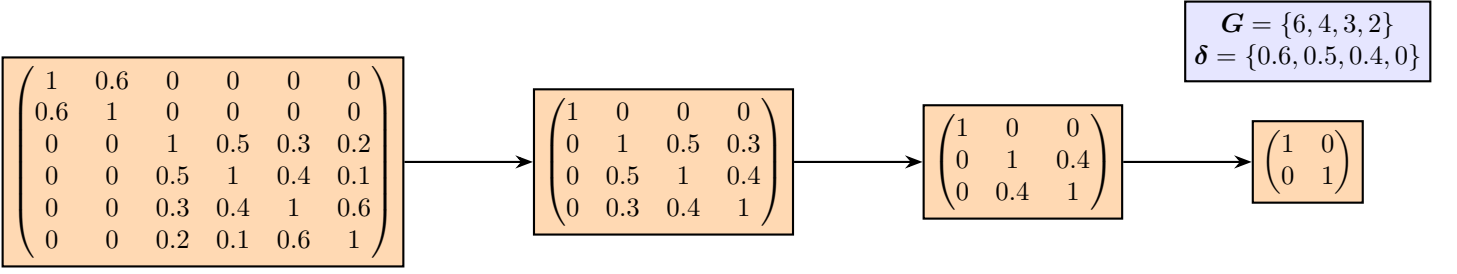


Fig. 5: A toy example illustrating the hierarchical structure in grouping filtered centers, alongside the relationship between the threshold δ and the number of groups G . This process generates two lists, G and δ , which store the number of groups and the corresponding threshold values at each stage, respectively. The elements of these lists are displayed in the top right.

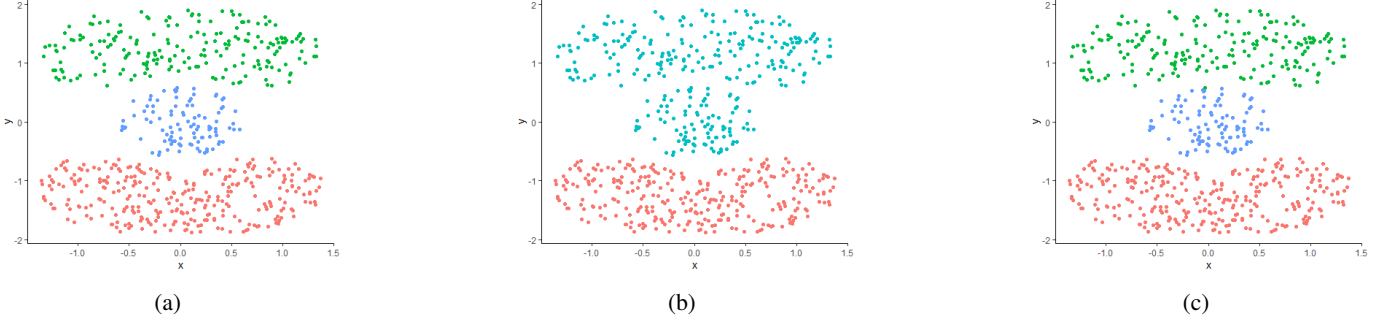


Fig. 6: Clustering results for the synthetic dataset Bainba. Panel (a) shows the ground truth, (b) merges two distinct clusters into one, and (c) incorrectly clusters a point at the top of the central elliptical cluster.

accommodate various forms of similarity matrices, \mathbb{S} . Some definitions from DBCA are listed below:

Definition 6 (Core Neighbors). *Given a depth similarity threshold η , a point \mathbf{x}_j is a core neighbor of \mathbf{x}_i (with respect to η) if $\mathbb{S}_{ij} \geq \eta$.*

Definition 7 (Depth-Connection). *A point \mathbf{x}_u is depth-connected to \mathbf{x}_v if there is a chain of points $\tilde{\mathbf{x}}_1, \dots, \tilde{\mathbf{x}}_i$, where each two adjacent points are core neighbors for each other, $\tilde{\mathbf{x}}_1 = \mathbf{x}_u$, and $\tilde{\mathbf{x}}_i = \mathbf{x}_v$.*

Definition 8 (DBCA-Cluster). *A chain $\mathbf{V} = \{\tilde{\mathbf{x}}_1, \dots, \tilde{\mathbf{x}}_i\}$ is called a maximal depth-connected chain if there is no $\mathbf{x}_j \notin \mathbf{V}$ satisfying $\sup_{\mathbf{x}_i \in \mathbf{V}} \mathbb{S}_{ij} \geq \eta$. Let \tilde{n} be the minimum number of points required to form a cluster in DBCA, then each cluster is formed by observations that are in the same maximal depth-connected chain with length at least \tilde{n} .*

Definition 9 (Outliers). *All observations that remain unlabelled in DBCA are regarded as outliers.*

In Definition 6, larger η corresponds to fewer core neighbors, which corresponds to a smaller fixed region. Let η_X be the largest value of η such that all observations in the dataset are depth-connected. Let k be the label of a cluster in the clustering result which is to be examined by the DC metric, and η_k be the maximum η value such that the cluster is decomposed into a single DBCA-cluster and outliers (without considering observations in other clusters). Let \mathcal{X}_k be the set of observations in cluster k . Let $n_k = |\mathcal{X}_k|$ and \mathbf{O}_k be the set of DBCA-outliers. For each observation $\mathbf{x}_i \in \mathcal{X}_k$, we define $\mathcal{J}_k^i = \{j | \mathbf{x}_j \in \mathcal{X}_k, \mathbf{x}_j \neq \mathbf{x}_i, \mathbb{S}_{ij} > \eta_k\}$ as the set of indices.

Following this, the within cluster similarity J_k of cluster k is defined by

$$J_k = \sum_{i=1}^{n_k} w_i \mu_i,$$

where

$$\mu_i = \begin{cases} \frac{\sum_{j \in \mathcal{J}_k^i} \mathbb{S}_{ij}}{|\mathcal{J}_k^i|}, & \text{if } \mathbf{x}_i \notin \mathbf{O}_k, \\ \max\{\mathbb{S}_{ij} | \mathbf{x}_j \in \mathcal{X}_k \setminus \mathbf{O}_k\}, & \text{if } \mathbf{x}_i \in \mathbf{O}_k, \end{cases}$$

$$w_i = \begin{cases} \frac{|\mathcal{J}_k^i|}{\sum_{\mathbf{x}_v \in \mathcal{X}_k \setminus \mathbf{O}_k} |\mathcal{J}_k^v| + |\mathbf{O}_k|}, & \text{if } \mathbf{x}_i \notin \mathbf{O}_k, \\ \frac{1}{\sum_{\mathbf{x}_v \in \mathcal{X}_k \setminus \mathbf{O}_k} |\mathcal{J}_k^v| + |\mathbf{O}_k|}, & \text{if } \mathbf{x}_i \in \mathbf{O}_k. \end{cases}$$

The weights w_i in J_k give observations with more core neighbors more weight and give outliers less weight. By considering DBCA-outliers, the DC metric can be made more robust by avoiding the significant adverse impact of an individual outlier.

For the cluster k , the set of inner observations is

$$\mathbf{I}_k := \{\mathbf{x}_i \in \mathcal{X}_k : \mathbb{S}_{ij} < \eta_X \text{ for all } \mathbf{x}_j \in \mathbf{X} \setminus \mathcal{X}_k\},$$

where \mathbf{X} is the total dataset. If $\mathbf{x}_i \in \mathbf{I}_k$ then \mathbf{x}_i is called an inner observation of cluster k , i.e., observations in \mathcal{X}_k that are not similar to any observation outside of \mathcal{X}_k . For defining the between cluster similarity H_k of cluster k , we set $\mathcal{H}_k^i = \{h | \mathbf{x}_h \notin \mathcal{X}_k, \mathbb{S}_{ih} > \eta_X\}$ to include indices of observations from other clusters that are core neighbors of points in \mathcal{X}_k .

when $\eta = \eta_X$. H_k is then defined as

$$H_k = \sum_{i=1}^{n_k} \tilde{w}_i \tilde{\mu}_i,$$

where,

$$\tilde{\mu}_i = \begin{cases} \frac{\sum_{h \in \mathcal{H}_k^i} S_{ih}}{|\mathcal{H}_k^i|}, & \text{if } \mathbf{x}_i \notin \mathbf{I}_k, \\ \eta_X, & \text{if } \mathbf{x}_i \in \mathbf{I}_k, \end{cases}$$

$$\tilde{w}_i = \begin{cases} \frac{|\mathcal{H}_k^i|}{\sum_{\mathbf{x}_u \in \mathcal{X}_k \setminus \mathbf{I}_k} (|\mathcal{H}_k^u| + |\mathbf{I}_k|)}, & \text{if } \mathbf{x}_i \notin \mathbf{I}_k, \\ \frac{1}{\sum_{\mathbf{x}_u \in \mathcal{X}_k \setminus \mathbf{I}_k} (|\mathcal{H}_k^u| + |\mathbf{I}_k|)}, & \text{if } \mathbf{x}_i \in \mathbf{I}_k. \end{cases}$$

In H_k , the weights \tilde{w}_i give observations which are close to other clusters more weight, but less weight for inner observations.

The total DC metric for a clustering result is then given by

$$\text{DC} = \sum_k \frac{n_k}{n} (J_k - H_k), \quad (20)$$

which gives more weight to the clustering performance in clusters with more observations. Some properties of the DC metric are summarized as follows:

- Property 1: For each observation $\mathbf{x}_i \in \mathcal{X}_k$, reducing the threshold from η_k to η_{k^*} implies $\mu_{i^*} \leq \mu_i$.
- Property 2: For each observation $\mathbf{x}_i \in \mathcal{X}_k$, reducing the threshold from η_k to η_{k^*} implies $\tilde{\mu}_{i^*} \leq \tilde{\mu}_i$.
- Property 3: For any cluster k , the μ_i given by any outlier is less than η_k .
- Property 4: For any cluster k , $H_k \geq \eta_X$, higher proportions of inner observations in k leads to smaller H_k .

Table III displays the DC metrics for the aforementioned clustering results for the Bainba and SmileyF datasets. Notably, the ranking of these scores aligns more closely with human assessments. Thus, using the DC metric allows for the selection of the parameters for the DLCC algorithm under the max strategy.

TABLE III: The DC metrics for clustering results in Figures 6 and 1, where $\tilde{n} = 3$. Note this score correctly assesses (a) as the best assignment of labels among the three panels.

	(a)	(b)	(c)
Bainba	0.046	0.044	0.045
SmileyF	0.174	0.164	0.079

V. EXPERIMENTS AND EVALUATIONS

In this section, we evaluate the performance of DLCC under various strategies, comparing it with several other clustering algorithms on both synthetic and real-world datasets.

External Metric. To compare the performance of different clustering algorithms on the same datasets, we use the clustering error (CE) [28, p. 2774] and adjusted Rand index (ARI) [51]. The CE simply computes the proportion of mismatched

points. This makes CE intuitive, with a value range of 0 (perfect match) to 1. The ARI, on the other hand, measures pairwise similarity between clustering results and ground truth. The expected value for the ARI under random class assignment is 0 and it takes a value 1 under perfect agreement.

Methods for comparison. We compare our approach with several representative clustering methods. These include the center-based algorithm K-means and its state-of-the-art variant LW-K-means; the recent advanced DPC method R-MDPC; the subspace clustering algorithm SSC; the model-based clustering algorithm GMM (GPCM family);

A. Description of Datasets

Figure 7 presents four synthetic datasets. The first subfigure is simulated using custom code, while the second and third subfigures are generated with the `mlbench` [53] package in R [52]. The last subfigure provides a two-dimensional visualization of the ray shapes data, which is derived from a study on spectral clustering [54]. These synthetic datasets represent different clustering scenarios with non-convex shapes, clusters of varying sizes and densities in close proximity, and large overlapping regions. Each of these characteristics presents unique challenges for clustering.

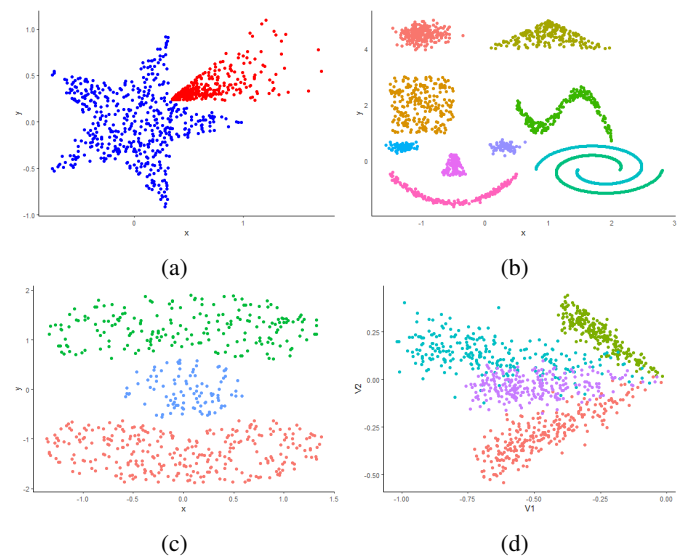


Fig. 7: Graphs of synthetic datasets: (a) Starbeam; (b) Blend; (c) Bainba; (d) Ray [54]. In (d), x and y axes are the first two variables of ray data. Colors represent true labels.

As for the real-world datasets, we utilize five benchmark datasets from the UCI Machine Learning Repository [55]: iris, seed, wine, optdigits, pendigits. Additionally, we test high-dimensional datasets ($d \geq 100$) with $n > d$, including Yale B [56] and HAR [57], which represent human-face and human-activity datasets, respectively, addressing clustering problems in different domains. Among these, Yale B, optdigits, and pendigit are sourced from the R package `PPCI` [58]. Furthermore, we consider two microarray datasets: leukemia [59] and SuCancer [60], which have large dimensions d but small sample sizes n .

B. Result comparisons

Table IV provides the settings, used for running DLCC on the above-mentioned datasets. The max strategy tends to perform better with non-convex or unbalanced sized clusters. Conversely, the min strategy is more effective for overlapping clusters of similar sizes.

TABLE IV: DLCC settings for different datasets, where CM stands for classification method.

Datasets	Depth	Strategy	CM	maxdepth	ifloop
Starbeam	MD	Max	KNN	False	–
Starbeam	SD	Max	KNN	False	–
Blend	MD	Max	KNN	False	–
Blend	SD	Max	KNN	False	–
Bainba	MD	Max	MDC	True	–
Bainba	SD	Max	KNN	False	–
Ray	MD	Min	MDC	False	True
Ray	SD	Min	RF	False	False
Iris	MD	Min	MDC	True	False
Iris	SD	Min	RF	False	False
Seed	MD	Min	KNN	True	True
Seed	SD	Min	KNN	False	False
Wine	MD	Min	MDC	True	True
Wine	SD	Min	MDC	False	False
Yale B	SD	Min	RF	False	False
Optidigit	SD	Min	KNN	False	False
Pendigits	MD	Min	KNN	False	False
Pendigits	SD	Min	KNN	False	False
HAR	SD	Min	KNN	False	False
Leukemia	SD	Max	MDC	False	–
SuCancer	SD	Max	RF	False	–

Table V illustrates the performance of DLCC with both MD and SD, compared to other clustering algorithms. For all comparing methods, we pick the result achieving the highest ARI as the best. For K-means and LW-K-means, we report the best results from 10 runs. For the R-MDPC method, following the suggestions, we fix $cv = 1$ and test all neighborhood sizes from $0.5\sqrt{n}$ to $2\sqrt{n}$ [18]. For SSC, the best combinations are chosen with regards to the hyper parameter α (ranging from 10 to 50 with a step size of 10) and the logical parameters “affine” (indicating if affine subspaces are considered) and “outlier” (signifying if the data might be contaminated by outliers). In the case of GMM, the R package `mixture` [61] is used to identify the optimal model from the GPCM family. As for DLCC, when RF is employed as the classification method, its inherent randomness led us to conduct 100 separate runs with unique seeds. The corresponding internal metric for each run was calculated, and the median performance score was recorded in the table.

Table V clearly demonstrates that DLCC yields impressively competitive results across all datasets. Specifically, in the synthetic datasets, both versions of DLCC perform perfectly in Starbeam and Bainba, while they meet some challenges in

Blend. As detailed in Section III-A, the max strategy assumes that, within any given cluster, each subset used for defining local centers is convex. Although the filtering procedures for local centers can identify the areas of non-convex subsets, they are unable to further distinguish individual clusters within these regions and, in the current context, to identify the two distinct spirals. DLCC_{MD} achieves the best performance on the Ray dataset, closely matching that of GMM, as its similarity matrix is constructed based on the EEV model, a member of GMM. DLCC_{SD} proves highly adaptable for high-dimensional data applications, delivering the best results in the Yale B and Leukemia datasets and ranking among the top performers on other high-dimensional datasets. In contrast, each of the other algorithms displays distinct strengths and limitations. For instance, K-means and LW-Kmeans produce satisfactory results for convex datasets, while they do not perform well on datasets with non-convex shapes. R-MDPC performs well on non-convex datasets and excels on the Optidigits dataset. However, it faces challenges with datasets that have large overlapping regions with similar densities, such as Ray and HAR. SSC excels with high-dimensional datasets but falters when the dimension d is less than or close to the number of clusters K . Both GMM and DLCC_{MD} face challenges in high-dimensional data due to their reliance on covariance matrix estimations. Accurately estimating covariance matrices requires significantly more observations per cluster than the number of dimensions, which is often not feasible for high-dimensional data.

C. Performance in estimating the number of cluster

For the max strategy, the relationship between δ and the number of clusters is detailed in Section IV. Here, we evaluate the effectiveness of Algorithm 1 in estimating the number of clusters under the min strategy. To ensure a fair comparison, the results presented in Table V assume that the true number of clusters is known. In this section, we focus on the scenario where K is not pre-specified, specifically discussing DLCC_{SD} as it is applicable to all datasets.

To provide insights into the performance of our method, we compare it with a well-established spectral clustering method, Spectrum [62], which can automatically estimate the number of clusters during the clustering process without requiring extensive parameter tuning. The implementation of Spectrum is based on the R package `Spectrum` [63], and we report the better results between the eigengap method (largest gap between eigenvalues) and the multimodality gap method.

Table VI demonstrates that without pre-defined K , DLCC_{SD} consistently outperforms Spectrum in terms of ARI. Although DLCC_{SD} estimates two additional clusters in the Pendigits dataset, its ARI is even higher compared to the scenario where K is fixed at 10. For the Optidigits and HAR datasets, DLCC_{SD} underestimates the number of clusters by one. Specifically, it merges clusters “3” and “8” into a single cluster in Optidigits, and in HAR, it groups walking, walking upstairs, and walking downstairs into one cluster. This clustering also makes sense based on human assessments.

TABLE V: Comparative analysis of selected clustering algorithms on several datasets (“–” means a method is not applicable).

Datasets	Metric	DLCC _{MD}	DLCC _{SD}	Kmeans	LW-Kmeans	SSC	GMM	R-MDPC
Starbeam $n = 780, d = 2, K = 2$	ARI	1	1	0.4822	0.4822	0.3052	0.0157	0.8123
	CE	0	0	15.26%	15.26%	22.31%	40.26%	4.87%
Blend $n = 2000, d = 2, K = 10$	ARI	0.8595	0.8605	0.7266	0.7365	0.5716	0.7518	0.8453
	CE	12.50%	8.65%	25.70%	18.90%	31.35%	21.45%	9.10%
Bainba $n = 600, d = 2, K = 3$	ARI	1	1	0.4961	0.9814	0.4276	0.7436	1
	CE	0	0	32.00%	0.67%	30.17%	10.50%	0
Ray $n = 1000, d = 5, K = 4$	ARI	0.8261	0.7521	0.6388	0.7090	0.7081	0.8245	0.5364
	CE	7.00%	10.00%	15.00%	11.90%	12.60%	7.10%	37.70%
Iris $n = 150, d = 4, K = 3$	ARI	0.9039	0.8857	0.7302	0.8857	0.6138	0.9039	0.8857
	CE	3.33%	4.00%	10.67%	4.00%	17.33%	3.33%	4.00%
Seed $n = 210, d = 7, K = 3$	ARI	0.7612	0.7626	0.7167	0.6687	0.4462	0.6299	0.7289
	CE	8.57%	8.57%	10.48%	12.86%	33.33%	14.76%	10.00%
Wine $n = 178, d = 13, K = 3$	ARI	0.9817	0.9295	0.8975	0.8516	0.8804	0.9309	0.7269
	CE	0.56%	2.25%	3.37%	5.06%	3.93%	2.25%	9.66%
Yale B $n = 2000, d = 600, K = 10$	ARI	–	0.9901	0.5663	0.8461	0.9484	–	0.7635
	CE	–	0.45%	31.85%	13.25%	2.40%	–	12.10%
Optidigits $n = 5620, d = 64, K = 10$	ARI	–	0.8144	0.5682	0.5799	0.7540	0.4878	0.8543
	CE	–	9.40%	28.81%	28.26%	14.84%	36.89%	8.75%
Pendigits $n = 10992, d = 16, K = 10$	ARI	0.6488	0.6661	0.5526	0.5756	0.7069	0.6522	0.6657
	CE	20.52%	18.22%	32.25%	27.83%	15.56%	20.58%	19.17%
HAR $n = 10299, d = 561, K = 6$	ARI	–	0.6564	0.4610	0.4556	0.7005	–	0.4373
	CE	–	18.68%	40.00%	41.51%	23.11%	–	51.06%
Leukemia $n = 72, d = 3571, K = 2$	ARI	–	0.8897	0.8897	0.8897	0.7371	–	0.7851
	CE	–	2.78%	2.78%	2.78%	6.94%	–	5.56%
SuCancer $n = 174, d = 7909, K = 2$	ARI	–	0.1154	–0.003	–0.003	0.1234	–	0.1154
	CE	–	32.76%	47.70%	47.70%	32.18%	–	32.76%

TABLE VI: Comparison of performance between DLCC_{SD} and Spectrum across datasets. Here, \hat{K} denotes the estimated number of clusters, with differences from true K in parentheses.

Method	Ray		Iris		Seed		Wine		Yale B		Optidigits		Pendigits		HAR	
	\hat{K}	ARI	\hat{K}	ARI	\hat{K}	ARI	\hat{K}	ARI								
DLCC _{SD}	4 (0)	0.7521	3 (0)	0.8857	3 (0)	0.7626	3 (0)	0.9295	10 (0)	0.9901	9 (–1)	0.7174	12 (+2)	0.6885	4 (–2)	0.4813
Spectrum	3 (–1)	0.6468	3 (0)	0.8508	3 (0)	0.5702	3 (0)	0.9170	9 (–1)	0.7575	9 (–1)	0.6527	10 (0)	0.5086	10 (+4)	0.3242

D. Complexity Analysis

The computational cost of the DLCC algorithm is dominated by constructing the depth-based similarity matrix and estimating local centers. For both versions, the first term corresponds to constructing the similarity matrix, and the second term accounts for estimating local centers, with $s \ll n$.

- **DLCC_{MD}**: With pre-estimated covariance matrices (Section II-B), the complexity is $O(n^2) + O(ns^2 + ns)$, where $O(ns^2 + ns)$ covers covariance matrix estimation and depth computation for neighborhoods. As $s \ll n$, the overall complexity simplifies to $O(n^2)$.
- **DLCC_{SD}**: The complexity is $O(n^3) + O(ns^2)$. Construct-

ing the similarity matrix requires $O(n^3)$, as computing SD values for n points ($O(n^2)$) across n reflected datasets introduces an additional n factor. Estimating local centers for neighborhoods adds $O(ns^2)$, resulting in an overall complexity of $O(n^3)$.

Figure 8a shows that the experimental running times align with theoretical complexities: $O(n^2)$ for DLCC_{MD} and $O(n^3)$ for DLCC_{SD}. In Figure 8b, the running time of DLCC_{MD} appears irregular as dimensionality increases because when estimating the covariance matrix, the method defaults to the identity matrix if singularity issues arise, which are more likely when the dimensionality is not significantly smaller than the

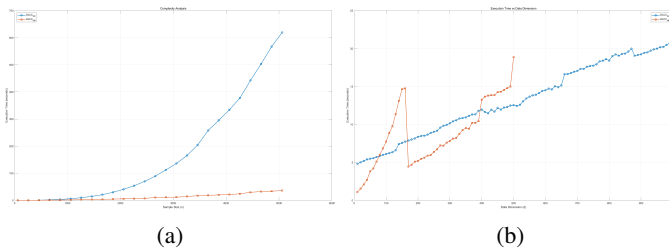


Fig. 8: Running time of DLCC on simulated datasets without acceleration techniques, where blue represents DLCC_{SD} and red represents DLCC_{MD}: (a) Fixed the dimension at 30 while increasing the sample size up to 5060, y-axis up to 700s; (b) Fixed the sample size at 1000 while increasing the dimension up to 1000, y-axis up to 25s.

sample size. In contrast, DLCC_{SD} shows a linear trend due to the SD computation involving the L^2 norm of the average of unit vectors, with a complexity of $O(n^3d)$ when d is large.

While DLCC can handle datasets with approximately 10,000 samples, its computational cost is dominated by the depth-based similarity matrix, limiting its scalability to larger datasets. However, DLCC_{SD} is computationally efficient with increasing dimensionality. Future work could explore approximation methods to accelerate the algorithm. For instance, defining local centers does not necessarily require computing the entire similarity matrix but rather identifying suitable neighborhoods for the centers. Fast approximate neighborhood search methods (e.g., [64]) could be employed to estimate candidate local centers (with size much smaller than n), followed by exact depth similarity computations for points relative to these candidates.

VI. CONCLUSIONS AND FUTURE WORK

In this paper, we have proposed an innovative clustering framework, DLCC, which first defines a depth-based similarity matrix to provide orderings of neighbors for each observation. DLCC then uses depth to define representative points, or “local centers”, with the number of these local centers controlled by the parameter indicating the neighborhood size, s . Our results show that DLCC delivers superior clustering performances under a wide range of scenarios. This includes handling both convex and non-convex shapes, managing clusters of balanced and unbalanced sizes, working with well-separated and overlapping clusters, and analyzing clustering problems in both low and high-dimensional spaces, including datasets with small n and large d .

For future research, a key direction is to develop an efficient DLCC method for handling larger datasets. Moreover, while this paper focuses on MD and SD for their computational simplicity, exploring other depth definitions, such as the integrated rank-weighted depth [65], could further enhance the DLCC framework. Furthermore, as depth is also a well-defined concept for functional data, e.g., band depth [66], there are many potential avenues for extending the DLCC framework to functional data analysis.

ACKNOWLEDGMENTS

This work is supported by the Canada Research Chairs program (PM), a Dorothy Killiam Fellowship (PM), and respective NSERC Discovery Grants (AL, PM).

REFERENCES

- [1] A. K. Jain and R. C. Dubes, *Algorithms for Clustering Data*. Englewood Cliffs, NJ: Prentice-Hall, 1988.
- [2] D. Xu and Y. Tian, “A comprehensive survey of clustering algorithms,” *Annals of Data Science*, vol. 2, pp. 165–193, 2015.
- [3] A. K. Jain, M. N. Murty, and P. J. Flynn, “Data clustering: a review,” *ACM Computing Surveys (CSUR)*, vol. 31, no. 3, pp. 264–323, 1999.
- [4] A. K. Jain, “Data clustering: 50 years beyond K-means,” *Pattern Recognition Letters*, vol. 31, no. 8, pp. 651–666, 2010.
- [5] W. Hu, X. Xiao, Z. Fu, D. Xie, T. Tan, and S. Maybank, “A system for learning statistical motion patterns,” *IEEE Transactions on Pattern Analysis and Machine Intelligence*, vol. 28, no. 9, pp. 1450–1464, 2006.
- [6] A. Y. Yang, J. Wright, Y. Ma, and S. S. Sastry, “Unsupervised segmentation of natural images via lossy data compression,” *Computer Vision and Image Understanding*, vol. 110, no. 2, pp. 212–225, 2008.
- [7] R. Tron and R. Vidal, “A benchmark for the comparison of 3-D motion segmentation algorithms,” in *2007 IEEE conference on computer vision and pattern recognition*. IEEE, 2007, pp. 1–8.
- [8] P. Sharma and J. Suji, “A review on image segmentation with its clustering techniques,” *International Journal of Signal Processing, Image Processing and Pattern Recognition*, vol. 9, no. 5, pp. 209–218, 2016.
- [9] J. MacQueen, “Some methods for classification and analysis of multivariate observations,” in *Proceedings of the Fifth Berkeley Symposium on Mathematical Statistics and Probability*, vol. 1, no. 14, Oakland, CA, USA, 1967, pp. 281–297.
- [10] L. Kaufman and P. J. Rousseeuw, “Finding groups in data: An introduction to cluster analysis,” 1990.
- [11] J. Z. Huang, M. K. Ng, H. Rong, and Z. Li, “Automated variable weighting in k-means type clustering,” *IEEE Transactions on Pattern Analysis and Machine Intelligence*, vol. 27, no. 5, pp. 657–668, 2005.
- [12] S. Chakraborty and S. Das, “Detecting meaningful clusters from high-dimensional data: A strongly consistent sparse center-based clustering approach,” *IEEE Transactions on Pattern Analysis and Machine Intelligence*, vol. 44, no. 6, pp. 2894–2908, 2020.
- [13] J. Xu and K. Lange, “Power k-means clustering,” in *International Conference on Machine Learning*. PMLR, 2019, pp. 6921–6931.
- [14] D. Paul, S. Chakraborty, S. Das, and J. Xu, “Implicit annealing in kernel spaces: A strongly consistent clustering approach,” *IEEE Transactions on Pattern Analysis and Machine Intelligence*, 2022.
- [15] M. Ester, H.-P. Kriegel, J. Sander, X. Xu et al., “A density-based algorithm for discovering clusters in large spatial databases with noise,” in *Proceedings of 2nd International Conference on Knowledge Discovery and Data Mining (KDD-96)*, vol. 96, no. 34, 1996, pp. 226–231.
- [16] Y. Rani and H. Rohil, “A study of hierarchical clustering algorithm,” *International Journal of Information and Computation Technology*, vol. 3, no. 11, pp. 1225–1232, 2013.
- [17] A. Rodriguez and A. Laio, *Clustering by fast search and find of density peaks*. American Association for the Advancement of Science, 2014, *Science*, vol. 344, no. 6191, pp. 1492–1496.
- [18] J. Guan, S. Li, J. Zhu, X. He, and J. Chen, *Fast main density peak clustering within relevant regions via a robust decision graph*. Elsevier, 2024, *Pattern Recognition*, vol. 152, p. 110458.
- [19] P. D. McNicholas, “Model-based clustering,” *Journal of Classification*, vol. 33, pp. 331–373, 2016.
- [20] T. I. Lin, “Maximum likelihood estimation for multivariate skew normal mixture models,” *Journal of Multivariate Analysis*, vol. 100, no. 2, pp. 257–265, 2009.
- [21] B. C. Franczak, R. P. Browne, and P. D. McNicholas, “Mixtures of shifted asymmetric Laplace distributions,” *IEEE Transactions on Pattern Analysis and Machine Intelligence*, vol. 36, no. 6, pp. 1149–1157, 2014.
- [22] R. P. Browne and P. D. McNicholas, “A mixture of generalized hyperbolic distributions,” *Canadian Journal of Statistics*, vol. 43, no. 2, pp. 176–198, 2015.
- [23] Y. Wei, Y. Tang, and P. D. McNicholas, “Flexible high-dimensional unsupervised learning with missing data,” *IEEE Transactions on Pattern Analysis and Machine Intelligence*, vol. 42, no. 3, pp. 610–621, 2020.
- [24] A. P. Dempster, N. M. Laird, and D. B. Rubin, “Maximum likelihood from incomplete data via the EM algorithm,” *Journal of the Royal Statistical Society: Series B*, vol. 39, no. 1, pp. 1–38, 1977.

- [25] A. Ng, M. Jordan, and Y. Weiss, "On spectral clustering: Analysis and an algorithm," *Advances in neural information processing systems*, vol. 14, 2001.
- [26] U. Von Luxburg, "A tutorial on spectral clustering," *Statistics and Computing*, vol. 17, pp. 395–416, 2007.
- [27] R. Vidal, "Subspace clustering," *IEEE Signal Processing Magazine*, vol. 28, no. 2, pp. 52–68, 2011.
- [28] E. Elhamifar and R. Vidal, "Sparse subspace clustering: Algorithm, theory, and applications," *IEEE Transactions on Pattern Analysis and Machine Intelligence*, vol. 35, no. 11, pp. 2765–2781, 2013.
- [29] J. W. Tukey, "Mathematics and the picturing of data," in *Proceedings of the International Congress of Mathematicians*, vol. 2, Vancouver, 1975, pp. 523–531.
- [30] Y. Zuo and R. Serfling, "General notions of statistical depth function," *The Annals of Statistics*, pp. 461–482, 2000.
- [31] K. Mosler and P. Mozharovskiy, *Choosing among notions of multivariate depth statistics*. Institute of Mathematical Statistics, 2022, *Statistical Science*, vol. 37, no. 3, pp. 348–368.
- [32] R. Jörnsten, "Clustering and classification based on the L1 data depth," *Journal of Multivariate Analysis*, vol. 90, no. 1, pp. 67–89, 2004.
- [33] M.-H. Jeong, Y. Cai, C. J. Sullivan, and S. Wang, "Data depth based clustering analysis," in *Proceedings of the 24th ACM SIGSPATIAL International Conference on Advances in Geographic Information Systems*, 2016, pp. 1–10.
- [34] A. Torrente and J. Romo, "Initializing k-means clustering by bootstrap and data depth," *Journal of Classification*, vol. 38, pp. 232–256, 2021.
- [35] J. Albert-Smet, A. Torrente, and J. Romo, "Band depth based initialization of k-means for functional data clustering," *Advances in Data Analysis and Classification*, pp. 1–22, 2022.
- [36] R. Serfling, "A depth function and a scale curve based on spatial quantiles," in *Statistical Data Analysis Based on the L1-Norm and Related Methods*. Springer, 2002, pp. 25–38.
- [37] D. Paindavein and G. Van Bever, "From depth to local depth: A focus on centrality," *Journal of the American Statistical Association*, vol. 108, no. 503, pp. 1105–1119, 2013.
- [38] D. Paindavein and G. Van Bever, "Nonparametrically consistent depth-based classifiers," *Bernoulli*, pp. 62–82, 2015.
- [39] X. Huang and Y. R. Gel, "Crad: clustering with robust autocuts and depth," in *2017 IEEE International Conference on Data Mining (ICDM)*. IEEE, 2017, pp. 925–930.
- [40] M. Hubert and M. Debruyne, "Minimum covariance determinant," *Wiley Interdisciplinary Reviews: Computational Statistics*, vol. 2, no. 1, pp. 36–43, 2010.
- [41] J. D. Banfield and A. E. Raftery, "Model-based Gaussian and non-Gaussian clustering," *Biometrics*, vol. 49, no. 3, pp. 803–821, 1993.
- [42] G. Celeux and G. Govaert, "Gaussian parsimonious clustering models," *Pattern Recognition*, vol. 28, no. 5, pp. 781–793, 1995.
- [43] P. D. McNicholas, *Mixture Model-Based Classification*. Boca Raton: Chapman and Hall/CRC Press, 2016.
- [44] G. Schwarz, "Estimating the dimension of a model," *The Annals of Statistics*, vol. 6, no. 2, pp. 461–464, 1978.
- [45] K. Pearson, "LIII. on lines and planes of closest fit to systems of points in space," *The London, Edinburgh, and Dublin Philosophical Magazine and Journal of Science*, vol. 2, no. 11, pp. 559–572, 1901.
- [46] R. G. Brereton, "The mahalanobis distance and its relationship to principal component scores," *Journal of Chemometrics*, vol. 29, no. 3, pp. 143–145, 2015.
- [47] L. Van der Maaten and G. Hinton, "Visualizing data using t-SNE," *Journal of Machine Learning Research*, vol. 9, no. 11, pp. 2579–2605, 2008.
- [48] S. Xu, X. Qiao, L. Zhu, Y. Zhang, C. Xue, and L. Li, "Reviews on determining the number of clusters," *Applied Mathematics & Information Sciences*, vol. 10, no. 4, pp. 1493–1512, 2016.
- [49] P. J. Rousseeuw, "Silhouettes: a graphical aid to the interpretation and validation of cluster analysis," *Journal of Computational and Applied Mathematics*, vol. 20, pp. 53–65, 1987.
- [50] T. Caliński and J. Harabasz, "A dendrite method for cluster analysis," *Communications in Statistics – Theory and Methods*, vol. 3, no. 1, pp. 1–27, 1974.
- [51] L. Hubert and P. Arabie, "Comparing partitions," *Journal of Classification*, vol. 2, no. 1, pp. 193–218, 1985.
- [52] R Core Team, "R: A Language and Environment for Statistical Computing," R Foundation for Statistical Computing, Vienna, Austria, 2021. [Online]. Available: <https://www.R-project.org/>
- [53] F. Leisch and E. Dimitriadou, *mlbench: Machine Learning Benchmark Problems*, 2021, r package version 2.1-3.
- [54] F. S. Passino, N. A. Heard, and P. Rubin-Delanchy, "Spectral clustering on spherical coordinates under the degree-corrected stochastic block-model," *Technometrics*, pp. 1–12, 2022.
- [55] D. Dua and C. Graff, "UCI machine learning repository," 2017. [Online]. Available: <http://archive.ics.uci.edu/ml>
- [56] A. S. Georghiadis, P. N. Belhumeur, and D. J. Kriegman, "From few to many: Illumination cone models for face recognition under variable lighting and pose," *IEEE Transactions on Pattern Analysis and Machine Intelligence*, vol. 23, no. 6, pp. 643–660, 2001.
- [57] D. Anguita, A. Ghio, L. Oneto, X. Parra, and J. L. Reyes-Ortiz, "A public domain dataset for human activity recognition using smartphones," in *The European Symposium on Artificial Neural Networks*, 2013. [Online]. Available: <https://api.semanticscholar.org/CorpusID:6975432>.
- [58] D. P. Hofmeyr and N. G. Pavlidis, "Ppci: an R package for cluster identification using projection pursuit," *The R Journal*, vol. 11, no. 2, pp. 152–170, 2019.
- [59] T. R. Golub, D. K. Slonim, P. Tamayo, C. Huard, M. Gaasenbeek, J. P. Mesirov, H. Coller, M. L. Loh, J. R. Downing, M. A. Caligiuri, C. D. Bloomfield, and E. S. Lander, "Molecular classification of cancer: class discovery and class prediction by gene expression monitoring," *Science*, vol. 286, no. 5439, pp. 531–537, 1999.
- [60] A. I. Su, J. B. Welsh, L. M. Sapinoso, S. G. Kern, P. Dimitrov, H. Lapp, P. G. Schultz, S. M. Powell, C. A. Moskaluk, H. F. Frierson Jr, and G. M. Hampton, "Molecular classification of human carcinomas by use of gene expression signatures," *Cancer Research*, vol. 61, no. 20, pp. 7388–7393, 2001.
- [61] N. Pocuca, R. P. Browne, and P. D. McNicholas, "mixture: Mixture Models for Clustering and Classification," R package version 2.1.1, 2024. [Online]. Available: <https://CRAN.R-project.org/package=mixture>
- [62] C. R. John, D. Watson, M. R. Barnes, C. Pitzalis, and M. J. Lewis, "Spectrum: fast density-aware spectral clustering for single and multi-omic data," *Bioinformatics*, vol. 36, no. 4, pp. 1159–1166, 2020.
- [63] C. R. John and D. Watson, "Spectrum: fast adaptive spectral clustering for single and multi-view data," R package version 1.1, 2020. [Online]. Available: <https://CRAN.R-project.org/package=Spectrum>.
- [64] C. Fu and D. Cai, "Efanna: An extremely fast approximate nearest neighbor search algorithm based on knn graph," *arXiv preprint arXiv:1609.07228*, 2016.
- [65] K. Ramsay, S. Durocher, and A. Leblanc, "Integrated rank-weighted depth," *Journal of Multivariate Analysis*, vol. 173, pp. 51–69, 2019.
- [66] S. López-Pintado and J. Romo, "On the concept of depth for functional data," *Journal of the American Statistical Association*, vol. 104, no. 486, pp. 718–734, 2009.